

## Implications of nucleon-nucleon spin-polarization measurements

E. L. Berger

*High Energy Physics Division, Argonne National Laboratory, Argonne, Illinois 60439*

A. C. Irving

*Department of Applied Mathematics and Theoretical Physics, University of Liverpool, Liverpool, England*

C. Sorensen

*High Energy Physics Division, Argonne National Laboratory, Argonne, Illinois 60439*

(Received 13 February 1978)

We discuss available data for spin observables in  $pp$  and  $np$  elastic scattering above 3 GeV/c. We identify those measurements which isolate exchange-amplitude components of specific interest—those which provide firm tests of Regge-exchange models and, on the other hand, those which models are unable to predict reliably. Using a simple Regge-pole-exchange model whose trajectory parameters and coupling properties are determined from data on other reactions, we compute expectations for all available  $pp$  spin observables and find good agreement with the data. We find that a hadronic axial-vector  $A_1$ -like exchange term is present in the data with strength compatible with theoretical estimates. The low-lying isoscalar exchange observed in  $pp$  and  $np$  polarization is consistent with estimates based on  $\epsilon(0^{++})$  exchange. We make a careful study of possible nonasymptotic Regge contributions which could obscure the interpretation of amplitude structure at momenta up to 6 GeV/c. We provide predictions for spin-correlation observables in  $np$  elastic and in  $np$  charge-exchange scattering.

### I. INTRODUCTION

Proton-proton elastic scattering is arguably the best measured and least understood high-energy scattering process. It has a large cross section and a beguiling simplicity fostered by its high degree of symmetry. This very simplicity, however, permits the exchange of every possible non-strange mesonic Regge pole, without restriction. Nonets of pseudoscalar, scalar, vector, tensor, axial-vector, and axial-tensor mesons, together with the Pomeron, are all potentially important. By comparison with  $\pi^+p \rightarrow \pi^0n$  charge exchange, in which only the  $\rho$  trajectory is involved out of the above long list of multiplets,  $pp$  scattering seems to be phenomenological chaos. Only if the nucleon spins can be controlled, is there much prospect of extracting useful information about exchange mechanisms or of testing models. With the aid of the ANL polarized proton beam facility, this is fortunately now possible, and complete knowledge of the  $pp \rightarrow pp$  amplitude structure at 6 GeV/c is no longer an idle dream.<sup>1,2</sup>

In anticipation of the expected amplitude analysis, it is useful to set up a simple model for the amplitude components to aid evaluation and interpretation of the results as they become available. In this paper, we present such a model and use it to interpret existing polarization information.

The dominance of  $pp \rightarrow pp$  by the Pomeron is a mixed blessing for the phenomenologist. On the one hand, it means that polarization and spin-

correlation coefficients are numerically small (and therefore hard to measure). On the other hand, one has the possibility of detecting small exchange components by *interference* with the Pomeron. Important information on the exchanges comes from studying  $pn$  elastic scattering for which polarization data are now available from 2 to 24 GeV/c. Together with our rough knowledge of the  $np$  charge-exchange amplitude structure, some constraint on the isospin of the exchanges is possible.

Separation of the exchanges according to parity (naturality) and  $C$  parity is partially possible using the double and triple spin measurements. We take advantage of these and the wide range of energies now spanned by much of the data (polarized-target data are now available from threshold up to 300 GeV/c) to separate the Pomeron, leading ( $\rho\omega A_2$ ) and low-lying Regge exchanges.

Since much of the current interest in  $pp$  scattering centers on low-lying natural- and unnatural-parity exchanges which are observable only at low energies ( $p_{lab} \leq 6$  GeV/c), we make a careful study of the correct Reggeization procedure and identify nonasymptotic contributions ( $\sim 1/s$ ) which could confuse the interpretation of such data.

The paper is organized as follows. In Sec. II, we define the amplitudes and their relationship to the observables used in the subsequent analysis. We discuss only those measurements which are actually being made<sup>1</sup> or are planned. The next section contains a description of the maximum-

simplicity model from which we start. This is followed in Sec. IV by our interpretation of the data using the model as a guide. Our suggestions for further experiments are listed in Sec. IV B, and concluding remarks are presented in Sec. V. The possible effects of nonleading Regge contributions are analyzed in Appendix A.

## II. AMPLITUDES AND POLARIZATION OBSERVABLES FOR $NN$ SCATTERING

We use the conventional  $s$ -channel helicity amplitudes  $\phi_1, \phi_2, \dots, \phi_5$  (Ref. 3) with invariant normalization,

$$\frac{d\sigma}{dt} = \frac{1}{2}K(|\phi_1|^2 + |\phi_2|^2 + |\phi_3|^2 + |\phi_4|^2 + 4|\phi_5|^2), \quad (1)$$

where

$$K = (0.3893/64\pi m_N^2 p_{1ab}^2) \text{ mb GeV}^{-2}, \quad (2)$$

with  $m_n$  in GeV and  $p_{1ab}$  in GeV/ $c$ . For convenience, we form combinations which asymptotically have definite exchange naturality,<sup>4,5</sup>

$$N_0 = \frac{1}{2}(\phi_1 + \phi_3), \quad N_2 = \frac{1}{2}(\phi_4 - \phi_2), \quad N_1 = \phi_5, \quad (3)$$

$$U_0 = \frac{1}{2}(\phi_1 - \phi_3), \quad U_2 = \frac{1}{2}(\phi_4 + \phi_2).$$

$N$  and  $U$  correspond respectively to  $t$ -channel natural- and unnatural-parity exchange. Their subscripts 0, 1, 2 refer to the total  $s$ -channel helicity flip involved ( $|\lambda_c - \lambda_a| + |\lambda_d - \lambda_b|$ ). The notation becomes obvious when the helicity labels for  $ab \rightarrow cd$  are exhibited on  $\phi_i$  explicitly,  $\phi_{\lambda_c \lambda_a \lambda_d \lambda_b}^{\lambda_c \lambda_a}$

$$\begin{aligned} \phi_1 &= \phi_{++}^{++}, & \phi_2 &= \phi_{--}^{--}, \\ \phi_3 &= \phi_{+-}^{+-}, & \phi_4 &= \phi_{-+}^{-+}, & \phi_5 &= \phi_{+-}^{+-}. \end{aligned} \quad (4)$$

Tabulations of all possible  $NN$  polarization measurements may be found in the literature.<sup>6</sup> A subset of these has been chosen for measurement at ANL<sup>1</sup> on grounds of practicality and maximum physics content. We limit our discussion to these. They can be classified as

- (a) Single-polarization measurement  $P$  (polarized beam or target),
  - (b) Total-cross-section measurements (polarized beam and target),
  - (c) Double-spin-correlation measurements: symbol C (polarized beam and target), symbol K (polarized beam and recoil), symbol D (polarized target and recoil),
  - (d) Triple-spin-correlation measurements H (polarized beam, target, and recoil).
- Their relationship to the  $N_m, U_m$  amplitudes is

TABLE I. Amplitudes and measurables for  $NN \rightarrow NN$ .

| Measurement   | Relation to amplitudes  |
|---|---|
| $\sigma \equiv \frac{d\sigma}{dt}$  | $K[ N_0 ^2 +  U_0 ^2 +  N_2 ^2 +  U_2 ^2 + 2 N_1 ^2]$   |
| $P\sigma$   | $-2K \text{Im}[(N_0 - N_2)N_1^*]$   |
| $\sigma_{\text{tot}}$   | $K' \text{Im}N_0$   |
| $\Delta\sigma_{\text{tot}}^T \equiv \sigma_{\text{tot}}(t+) - \sigma_{\text{tot}}(t-)$                  | $-K' \text{Im}\phi_2 = K' \text{Im}(N_2 - U_2)$   |
| $\Delta\sigma_{\text{tot}}^L \equiv \sigma_{\text{tot}}(\rightarrow) - \sigma_{\text{tot}}(\leftarrow)$ | $2K' \text{Im}U_0 \quad [K' = (0.3893/2m_N p_{1ab}) \text{ mb GeV}^{-2}]$   |
| $C_{NN}\sigma$  | $2K \text{Re}[U_0 U_2^* - N_0 N_2^* +  N_1 ^2]$   |
| $C_{LL}\sigma$  | $2K \text{Re}[N_2 U_2^* - N_0 U_0^*]$   |
| $C_{SS}\sigma$  | $2K \text{Re}[N_0 U_2^* - N_2 U_0^*]$   |
| $C_{SL}\sigma$  | $2K \text{Re}[(U_0 + U_2)N_1^*]$  |
| $K_{NN}\sigma$  | $-2K \text{Re}[U_0 U_2^* + N_0 N_2^* -  N_1 ^2]$  |
| $K_{SS}\sigma$  | $-2K \text{Re}[(U_2 - U_0)N_1^*] \sin\theta_R - 2K \text{Re}[N_0 U_2^* + N_2 U_0^*] \cos\theta_R$   |
| $D_{NN}\sigma$  | $K[ N_0 ^2 +  N_2 ^2 + 2 N_1 ^2 -  U_0 ^2 -  U_2 ^2]$   |
| $D_{SS}\sigma$  | $-2K \text{Re}[(N_0 + N_2)N_1^*] \sin\theta_R - K[ N_0 ^2 -  N_2 ^2 +  U_2 ^2 -  U_0 ^2] \cos\theta_R$  |
| $D_{LS}\sigma$  | $-2K \text{Re}[(N_0 + N_2)N_1^*] \cos\theta_R + K[ N_0 ^2 -  N_2 ^2 -  U_2 ^2 +  U_0 ^2] \sin\theta_R$  |
| $H_{LSN}\sigma$   | $2K \text{Im}[N_2 U_2^* - N_0 U_0^*]$   |
| $H_{NSS}\sigma$   | $2K \text{Im}[(N_0 + N_2)N_1^*] \cos\theta_R - 2K \text{Im}[U_0 U_2^* - N_0 N_2^*] \sin\theta_R$  |
| $H_{SNS}\sigma$   | $2K \text{Im}[(U_2 - U_0)N_1^*] \cos\theta_R + 2K \text{Im}[N_0 U_2^* + N_2 U_0^*] \sin\theta_R$  |
|   | $\theta_R = \text{lab recoil angle}$  |
|   | $\theta = \text{c.m.s. scattering angle}$   |
|   | $\left. \begin{array}{l} \theta_R = \text{lab recoil angle} \\ \theta = \text{c.m.s. scattering angle} \end{array} \right\} \tan\theta_R = \frac{2m_N}{\sqrt{s}} \cot(\frac{1}{2}\theta)$ |

TABLE II. Leading exchanges in  $pp$  scattering.

| Amplitude | Dominant contributions | Suppressed contributions |
|-----------|------------------------|--------------------------|
| $N_0$     | $P+f+\omega$           | $\rho+A_2$               |
| $N_2$     | $\rho+A_2$             | $P+f+\omega$             |
| $N_1$     | $\rho+A_2$             | $P+f+\omega$             |
| $U_0$     | $A_1+Z$                | $D+Z_0^a$                |
| $U_2$     | $\pi+B$                | $\eta+H^a$               |

<sup>a</sup> No firm evidence for these exchanges has yet been presented.

given in Table I. At 6 GeV/c, published data are available for the measurables  $d\sigma/dt$ ,<sup>7</sup>  $P$ ,<sup>8-11</sup>  $C_{NN}$ ,<sup>11,12</sup>  $C_{LL}$ ,<sup>13</sup>  $C_{SS}$ ,<sup>14</sup>  $C_{SL}$ ,<sup>15</sup>  $K_{NN}$ ,<sup>16</sup>  $D_{NN}$ ,<sup>17</sup>  $D_{SS}$ ,<sup>18</sup>  $D_{LS}$ ,<sup>1</sup>  $H_{SNS}$ ,<sup>1</sup>  $\Delta\sigma_{tot}^T$ ,<sup>19</sup> and  $\Delta\sigma_{tot}^L$ .<sup>13,20</sup>

The amplitudes  $N_0$ ,  $N_2$ , and  $N_1$  can each have Regge-pole contributions from the  $P$  (Pomeron),  $f$ ,  $\omega$ ,  $\rho$ , and  $A_2$  exchanges. Because of their known couplings to nucleons,<sup>21,22</sup> one expects  $N_0$  to be dominated by  $P$ ,  $f$ , and  $\omega$  while  $N_2$  should be largely due to  $\rho$  and  $A_2$  exchange. It is less easy to guess whether  $I=0$  or  $I=1$  exchange dominates  $N_1 = \phi_{\pm}^{*+}$  since both weak ( $I=0$  helicity flip,  $I=1$  helicity nonflip) and strong couplings ( $I=0$  helicity nonflip,  $I=1$  helicity flip) are involved. A combination of parity and  $G$  parity ensures that  $U_0$  and  $U_2$  are respectively due to  $A_1$ -like and  $\pi, B$  exchange respectively. These qualitative expectations are summarized in Table II.

From energy-dependent studies of  $d\sigma/dt$  and  $\sigma_T$ ,  $N_0$  (in particular, the Pomeron component) is known to be by far the largest amplitude and to be dominantly imaginary in phase, with  $\text{Re}N_0/\text{Im}N_0 < 0$  at  $t=0$ . According to Table II,  $N_2$  is dominantly  $I=1(\rho+A_2)$  and is therefore determined in magnitude by  $(d\sigma/dt)(np-pn)$ . Its phase is determined by the combination

$$(K_{NN} + C_{NN})\sigma = -4 \text{Re}(N_0 N_2^* - |N_1|^2). \quad (5)$$

The single-flip amplitude  $N_1$  is also accessible via its interference with  $N_0$ . Since  $N_0$  is largely imaginary, the quantity  $-(\sigma/4K)^{1/2}P$  determines  $\text{Re}N_1$  (presumably  $\text{Im}N_1$  is not large in view of approximate exchange degeneracy for  $\rho$ ,  $\omega$ ,  $f$ , and  $A_2$  and the small Pomeron flip coupling).

The amplitude  $U_2$ , dominated by  $\pi$  exchange, is reasonably well known from studies of  $np-pn$ . At  $t=0$  it has a strong cut contribution which interferes with the vanishing  $\pi$ -pole contribution [ $\propto -t/(t-\mu^2)$ ], giving rise to the observed forward spike. This cut, which also contributes to  $N_2$ , is expected to be approximately real. Any small imaginary part is observable in  $\Delta\sigma_{tot}^T = K' \text{Im}(N_2 - U_2)$  (Table I). The most direct mea-

sure of the amplitudes  $U_2$  and  $N_2$ , which are expected to be dominantly real, will be from  $H_{SNS}(\sim \text{Im}N_0 U_2^*)$  and  $H_{NSS}(\sim \text{Im}N_0 N_2^*)$  (see Table I).

The measurement  $\Delta\sigma_{tot}^L$  determines  $\text{Im}U_0(A_1+Z$  exchange). Crude exchange degeneracy predicts this to be small in comparison to  $\text{Re}U_0$  which, according to Table I, contributes significantly to  $C_{LL}(\sim -\text{Re}N_0 U_0^*)$  and to  $H_{LSN}(\sim -\text{Im}N_0 U_0^*)$ .

It is obvious from the above that, even in the absence of a complete  $t$ -dependent amplitude analysis, the experimental constraints on any model of the  $pp$  amplitude structure are already considerable. In the next section, we shall outline a simplified Regge-pole model for the helicity amplitude structure which incorporates the above prejudices quantitatively.

### III. SIMPLE REGGE-POLE MODEL FOR $pp$ AMPLITUDES

Because the  $pp$  system is generally accepted to be exotic, having no strong resonances,<sup>23</sup> Regge-pole-exchange contributions occur in exchange-degenerate pairs, their imaginary parts canceling. Except for the Pomeron terms, the exchange amplitudes are expected to be dominantly real. While imaginary parts may arise from various sources, such as broken exchange degeneracy and unitarity corrections, there is no good model for estimating their sizes and  $t$  dependences. The magnitudes, signs and  $t$  dependences of the real parts of the exchanges are reasonably well constrained theoretically, via pole extra-

TABLE III. Regge-pole parameters.

| Parameter   | Value              |
|---|--------------------|
| $\alpha_\rho = \alpha_\omega = \alpha_{A_2} = \alpha_f$ | $0.5 + 0.9t$       |
| $\alpha_P$  | $1 + 0.3t$         |
| $\alpha_\pi = \alpha_B$                                 | $0.9(t - m_\pi^2)$ |
| $\alpha_{A_1} = \alpha_Z$                               | $-0.19 + 0.9t$     |
| $\alpha_\epsilon = \alpha_{\omega'}$                    | $-0.5 + 0.9t$      |
| $\beta_{pp}^\rho = \beta_{pp}^{A_2}{}^{++}$             | 1.63               |
| $\beta_{pp}^\omega = \beta_{pp}^f{}^{++}$               | $10.6^a$           |
| $\beta_{pp}^\pi = \beta_{pp}^B{}^{+-}$                  | 1.9                |
| $\beta_{pp}^P$  | [See Eq. (9)]      |
| $\beta_{pp}^\pi = \beta_{pp}^B{}^{+-}$                  | 25.2               |
| $\beta_{pp}^{A_1} = \beta_{pp}^Z{}^{++}$                | 4.4                |
|   | (See Sec. III A)   |
| $\beta_{pp}^\epsilon = \beta_{pp}^{\omega'}{}^{++}$     | 20                 |
|   | -20                |
|   | (See Sec. III B)   |

<sup>a</sup> This value corresponds to  $F/D = -2.14$  rather than  $-3$  as quoted in Ref. 22. This has been adjusted to obtain the correct value of  $\sigma_{tot}(pp)$  while retaining a good description of the  $I=1$  exchanges.

polation, once dual residue functions are adopted. Thus, to the extent that our model is reliable, we expect to be successful in describing observables which are dominated by real parts of exchange amplitudes.

The specific model from which we start is the Regge-pole model of Ref. 22. It embodies all con-

straints due to factorization, SU(3) symmetry, and exchange degeneracy (EXD). This model, which has the acronym QUADREM, provides a crude overall description of the helicity structure and  $s, t$  dependence of most two-body processes. Each exchange contribution to the process  $ab \rightarrow cd$  is written as<sup>22</sup>

$$\phi_{\lambda_a \lambda_b}^{\lambda_c \lambda_d} = \mp (\sqrt{-t}/2m_N)^{|\lambda_c - \lambda_a|} (\sqrt{-t}/2m_N)^{|\lambda_d - \lambda_b|} \beta_{\lambda_c \lambda_a}^{\lambda_c \lambda_a} \beta_{\lambda_d \lambda_b}^{\lambda_d \lambda_b} \frac{1}{2} [1 + (-1)^{S_e} e^{-i\pi \alpha_e}] \Gamma(l_e - \alpha_e) (\alpha')^{1-l_e} (\alpha' s)^{\alpha_e}, \quad (6)$$

where  $S_e$  and  $l_e$  are respectively the spins of exchange  $e$  and of the lowest recurrence on the EXD trajectory  $\alpha_e(t)$ . The vertex parity ( $\eta$ ) relations are

$$\beta_{\lambda_a \lambda_b}^e = (-1)^{S_e} \eta_e \eta_c \eta_d (-1)^{S_d - \lambda_d - S_b + \lambda_b} \beta_{-\lambda_a - \lambda_b}^e. \quad (7)$$

Upper and lower vertices are related by<sup>24</sup>

$$\beta_{\lambda_a \lambda_b}^e = (-1)^{S_d - \lambda_d + S_b - \lambda_b} \beta_{\lambda_a \lambda_b}^e. \quad (8)$$

The residues  $\beta^e$  are simply related to coupling constants by evaluation of Eq. (6) near the pole,  $t = m_e^2$  ( $\alpha_e \approx S_e$ ). In the special case of elastic scattering where upper and lower vertices involve the same coupling constant, this enables a definite prediction of the amplitude's phase in terms of our extrapolation ansatz [Eq. (6)]. A careful study of pole extrapolations reveals that, except for the case of a natural-parity trajectory with lowest recurrence  $J^{PC} = 0^{++}$ , the appropriate sign in Eq. (6) is a minus sign if the residues  $\beta$  are taken to be real (i.e., only for the  $0^{++}$  case should it be a plus sign). Thus, for example, we find that, for  $\omega$  exchange,  $\text{Im} \omega < 0$  (and hence  $\text{Im} f > 0$ ) in  $N_0$  as, in fact, is required by the data.<sup>25</sup> As an illustration, in Sec. III A, we work through the case of  $A_1 + Z$  exchange which gives a real and negative contribution to  $U_0$ .

The actual values of  $\beta^e$  and  $\alpha_e$  are taken from the list of global-fit parameters given in Ref. 22 and are displayed in Table III.

For the Pomeron amplitude, we use an equally simple parametrization and fix its coupling by the assumption of  $f$  dominance.<sup>26</sup> We use<sup>27</sup>

$$\phi_{\lambda_a \lambda_b}^{\lambda_c \lambda_d} = -\frac{1}{2} x_P \sqrt{\pi} \beta_f^{\lambda_c \lambda_a} \beta_f^{\lambda_d \lambda_b} (-t/4m_N^2)^{(|\lambda_c - \lambda_a| + |\lambda_d - \lambda_b|)/2} \times e^{At} e^{-i\pi \alpha_P/2} (\alpha' s)^{\alpha_P}, \quad (9)$$

so that in each helicity amplitude,

$$(\text{Im} P / \text{Im} f) \Big|_{t=0} = x_P (\alpha' s)^{\alpha_P - \alpha_f}. \quad (10)$$

From  $\pi N$  elastic scattering data, one finds<sup>27</sup>  $x_P = 1.0$  and  $A = 2.5 \text{ GeV}^{-2}$ . For our  $pp$  case, we set

$$x_P = 1.0, \quad A = 3.1 \text{ GeV}^{-2}. \quad (11)$$

All absorption corrections are ignored except those in  $\pi$  (and  $B$ ) exchange amplitudes where they

are unavoidably present (they give the forward spike in  $np \rightarrow pn$ ). We use the Williams prescription<sup>28</sup> for applying these. Although this method has deficiencies, it has no free parameters and appears to mimic the correct amplitude structure in  $np \rightarrow pn$  up to quite high energies (30 GeV/c).<sup>29</sup> The procedure to obtain the absorbed  $\pi + B$  exchange amplitude is to make the replacement

$$(-t/4m_N^2)^{(n+x)/2} \rightarrow (-t/4m_N^2)^{n/2} (-m_\pi^2/4m_N^2)^{x/2}, \quad (12)$$

in Eq. 6 where  $n = |\lambda_c - \lambda_a - \lambda_d + \lambda_b|$  and  $n+x = |\lambda_c - \lambda_a| + |\lambda_d - \lambda_b|$ .

#### A. Regge-exchange contributions to $U_0$

The amplitude  $U_0$  contains the contributions of trajectories associated with particles of  $J^{PC} = 1^{++}$ ,  $3^{++} \dots$ , and  $J^{PC} = 2^{--}$ ,  $4^{--} \dots$ , i.e., with the  $A_1$  nonet,<sup>30</sup> and with the conjectured<sup>31</sup>  $Z(2^{--})$  nonet. The phase and magnitude of the  $A_1$ -exchange contribution to proton-proton elastic scattering can be estimated with some confidence, as we describe in detail in this subsection.<sup>32-35</sup> The  $Z$ -exchange contribution can then be inferred by invoking  $A_1$ - $Z$  exchange degeneracy, in agreement with experimental indications.<sup>36</sup> Furthermore, the contribution of the  $I=0$  partners of the  $A_1$  and  $Z$  can also be calculated given an  $F/D$  value for the coupling of these multiplets to  $N\bar{N}$ .

The estimate of the  $A_1$ -exchange contribution relies on standard assumptions about the  $t$  dependence of Regge residues, on vector- and axial-vector-meson dominance of the weak and electromagnetic currents, and on current algebra. Calculation of the overall sign of the contribution is made possible by the fact that we are dealing with elastic scattering of identical particles which couple in a unique way to a  $1^{++}$  meson. The calculation proceeds as follows: we first use the Feynman rules to compute the contribution of elementary  $A_1$  exchange to  $\phi_1$ . This allows us to determine the behavior of the corresponding invariant amplitude near the pole at  $t = m_{A_1}^2$ . Next we Reggeize the invariant amplitude in order to

extrapolate to the scattering region,  $t \leq 0$ .

In the high-energy limit, the Feynman rules yield

$$\phi_1 = \frac{(g_{A_1 \rho \bar{p}})^2}{t - m_{A_1}^2} (\bar{u}'_1 \gamma_\mu \gamma_5 u_{1+}) (\bar{u}'_2 \gamma_\mu \gamma_5 u_{2+}). \quad (13)$$

Reggeization of the invariant amplitude leads to

$$\frac{(g_{A_1 \rho \bar{p}})^2}{t - m_{A_1}^2} = \lim_{\alpha \rightarrow 1} \frac{(g_{A_1 \rho \bar{p}})^2}{\Gamma(\alpha)} \frac{\alpha' \pi}{\sin \pi \alpha} \frac{-1 + e^{-i\pi \alpha}}{2}. \quad (14)$$

In the last equation,  $\alpha$  denotes the  $A_1$  trajectory, which we assume to be linear. Also included is a factor  $1/\Gamma(\alpha)$  that provides the wrong signature zero required by duality and exchange degeneracy. (Some consequences of ignoring exchange degeneracy are discussed below.)

Evaluation of the spinor product in Eq. (13), Reggeization of the energy dependence, and rearrangement of the  $\Gamma$  functions in Eq. (14) finally yields

$$\begin{aligned} \phi_1^{A_1} &= -\phi_3^{A_1} \\ &= -(g_{A_1 \rho \bar{p}})^2 (\alpha' s)^{\alpha(t)} \Gamma(1 - \alpha(t)) (1 - e^{-i\pi \alpha(t)}). \end{aligned} \quad (15)$$

Comparison with Eq. (6) yields

$$(\beta_{++}^{A_1})^2 = 2(g_{A_1 \rho \bar{p}})^2.$$

The magnitude of the coupling constant  $g_{A_1 \rho \bar{p}} = (1/\sqrt{2})g_{A_1 \rho \bar{n}}$  can be estimated<sup>33,35</sup> if we assume vector-meson dominance of the vector and axial-vector weak currents:

$$C_A = (f_{A_1^+}/m_{A_1}^2) g_{A_1 \rho \bar{n}}. \quad (16)$$

This is analogous to the vector dominance of the  $\rho NN$  coupling,

$$\frac{1}{2} = (f_{\rho^+}/\sqrt{2}m_{\rho^2}) g_{\rho \bar{p} \bar{p}}. \quad (17)$$

In the above,  $C_A \approx 1.22$  is the value of the axial-vector form factor of the nucleon at  $t=0$ , as measured in  $\beta$  decay. The quantity  $g_{\rho \bar{p} \bar{p}}$  is defined by an equation identical to Eq. (13), but without the  $\gamma_5$  factors in the spinor product. The parameters  $f_{A_1^+}$ ,  $f_{\rho^+}$  denote the couplings of the  $A_1^+$  and  $\rho^+$  to the charged weak currents. Current-algebra considerations<sup>37</sup> provide

$$f_{\rho^+} = f_{A_1^+}. \quad (18)$$

Accepting this relation,<sup>38</sup> one finds

$$\frac{\beta_{A_1 \rho \bar{p}}}{\beta_{\rho \bar{p} \bar{p}}} = \frac{f_{\rho^+}}{f_{A_1^+}} \frac{m_{A_1}^2}{m_{\rho^2}} C_A \approx 2.78. \quad (19)$$

For  $\beta_{\rho \bar{p} \bar{p}}$  we use the value given in Table III, which is slightly different from that inferred from vec-

tor-meson dominance of the pion and nucleon form factors. Our procedure for normalizing  $\beta_{A_1 \rho \bar{p}}$  is not the same as the one described in Ref. 33 but the resulting numerical values are comparable.

For the mass of the  $A_1$  we have used  $m_{A_1} = 1.15$  GeV as suggested by the observed<sup>30</sup>  $\tau$  decay  $\tau \rightarrow A_1 \nu$ . For a linear trajectory with  $\alpha' = 0.9$  GeV<sup>-2</sup>, this value of the mass leads to

$$\alpha_{A_1}(t) = -0.19 + 0.9t. \quad (20)$$

As with other QUADREM estimates, the contribution of unnatural-parity exchanges to  $\phi_1$  and  $\phi_3$  is completed by the inclusion of the  $Z$  trajectory and of the corresponding  $I=0$  members of the  $1^{++}$  and  $2^{--}$  multiplets. Since  $pp$  is an exotic channel, the combination of  $A_1$  and  $Z$  exchanges must produce a real amplitude

$$U_0^{A_1-Z} = -2g_{A_1 \rho \bar{p}}^2 \Gamma(1 - \alpha_{A_1}(t)) (\alpha' s)^{\alpha(t)}. \quad (21)$$

Though nothing is known about the  $I=0$  partners of the  $A_1$  and  $Z$ , we include them by taking a canonical  $F/D = \frac{2}{3}$ , in analogy with the  $\pi$ - $B$  system. We include only the octet part of the exchanges.

We see that  $U_0$  is predicted to be real and negative at  $t=0$ . The measured value<sup>20</sup> of  $\Delta\sigma_L \cong -1$  mb for  $p_{lab} = 6$  GeV/ $c$  must be interpreted as a breaking of exchange degeneracy. This value of  $\Delta\sigma_L$  can be used to compute  $\text{Im}U_0$  at  $t=0$ . Comparison with the value of  $\text{Re}U_0$  calculated from Eq. (21) yields

$$\left| \frac{\text{Im}U_0}{\text{Re}U_0} \right| \approx 1. \quad (22)$$

Thus it appears that an approximately exchange degenerate pair of trajectories may not be the dominant exchange mechanism for  $U_0$ . To the extent that other known exchanges exist in approximately exchange degenerate pairs, this would point to yet another peculiarity of the  $A_1$  system.

We note that our  $A_1$ - $Z$ -exchange amplitude is nonvanishing at  $t=0$ . It was shown in Ref. 4 that a nonvanishing of the  $A_1$  coupling at  $t=0$  requires a "conspiracy." We demonstrate in Appendix B that the intercept of the conspirator (daughter) trajectory need be only  $\alpha_{A_1}(0) - 1$ . Since independent theoretical arguments for the existence of daughters are abundant, we believe there is no compelling reason to expect that  $\beta_{ppA_1}^{++}(t=0) = 0$ .

We remark that, once exchange degeneracy of the  $A_1$  and  $Z$  is abandoned, there is no need for the factor  $1/\Gamma(\alpha)$  in the  $A_1$  residue. With the trajectory function given in Eq. (20), absence of this zero implies that, in the scattering region,  $A_1$  exchange would give

$$\text{Im}U_0 < 0$$

and

$$\text{Im}U_0/\text{Re}U_0 = \cot\frac{1}{2}\pi\alpha < 0. \quad (23)$$

Thus  $\text{Re}U_0$  would be positive and small compared to  $\text{Im}U_0$ .

If degeneracy with the  $A_1$  is not used as a constraint, very little can be said about the contribution of  $Z$  exchange. If it dominates over  $A_1$  exchange, however, one should observe

$$\text{Im}U_0/\text{Re}U_0 = -\tan\frac{1}{2}\pi\alpha, \quad \text{Re}U_0 < 0. \quad (24)$$

A clean separation of the  $A_1$  and  $Z$  contribution would, of course, require spin measurements with antiproton beams. Similarly, separation of the  $I=0$  and  $I=1$  components would require  $\Delta\sigma_Z$  experiments with neutron beams.

Another source of departures from the simple result of Eq. (21) could be found in large absorptive corrections to such an amplitude. Naive absorption of Eq. (21) with a Pomeron amplitude yields a correction which is approximately real and of magnitude

$$\frac{U_0 \otimes P}{U_0} \approx -\frac{\beta_P^2}{8\pi} \frac{\exp\{-[b_A^2/(b_P + b_A)]t\}}{b_P + b_A},$$

with

$$\begin{aligned} b_P &\approx [3.1 + \alpha'_P \ln(\alpha's)] \text{ GeV}^{-2} \\ b_A &\approx [\alpha' \ln(\alpha's) + 0.58] \text{ GeV}^{-2} \end{aligned} \quad (25)$$

and

$$\beta_P^2 \approx 100 \text{ GeV}^{-2}.$$

Thus for  $p_{1ab} = 6 \text{ GeV}/c$ , we find

$$\frac{U_0 \otimes P}{U_0} \approx -0.6e^{-1.4t}. \quad (26)$$

We see that even though absorptive corrections could be quite large (as is always the case for  $n=0$  amplitudes), they are unlikely to change the sign of the real part at small values of  $t$ , and that

furthermore, they would not affect  $\text{Im}U_0$ .

Another source of contributions to  $U_0$  with an effective intercept  $\alpha \approx 0$  could be imagined to be in unitarity corrections generated by the overlap of two natural-parity-exchange amplitudes. It is a consequence of parity conservation, however, that such overlaps do not contribute to  $U_0$  at  $t=0$ , and can, therefore, be expected to be unimportant for small values of  $t$ .

We summarize the various alternatives described above in Table IV. We leave it to the reader to work out more perverse possibilities, e.g., badly broken EXD plus absorptive corrections.

Finally, a word must be said about our estimate of the magnitude of the  $A_1$ - $Z$  term. We feel that this is on less secure ground. For example, it is well known<sup>37</sup> that the same chiral-symmetry plus vector-dominance considerations that lead to the equality  $f_{A^+} = f_{\rho^+}$  (on which we rely), also predict a large width for  $A_1 \rightarrow \rho\pi$  (500 MeV). Since the observed width of the  $A_1$  appears to be between 200 and 450 MeV, we expect that the magnitude of our estimate for the  $A_1$ -exchange contribution is accurate to about a factor of 2.

#### B. $\epsilon$ -type exchange

Absence of mirror symmetry in  $pp$  and  $pn$  polarization measurements indicates the presence of an isoscalar exchange contribution to  $N_1$ . A study<sup>8</sup> of the energy dependence of the sum of the polarizations for  $pp$  and  $pn$  shows that the energy dependence of such an exchange is  $\sim s^{-0.5}$ . In this paper, we assume<sup>39</sup> that such an energy dependence is due to the exchange of a pair of exchange-degenerate trajectories  $\alpha_\epsilon(t) = -0.5 + 0.9t$  associated with particles of  $J^{PC} = 0^{++}, 1^{--}$ , and recurrences.

It has been noted before<sup>39</sup> that the empirical sign of this isoscalar-exchange contribution to  $N_1$  is the one expected from a  $J^{PC} = 0^{++}$  elementary exchange (the so-called scalar-exchange contribu-

TABLE IV. Possible signs for  $U_0$ . We have assumed  $\alpha_{A_1}(0) \leq 0$ ,  $\alpha_Z(0) \leq 0$ . Otherwise some signs should be reversed in lines 2 and/or 3. Line 2 assumes no wrong-signature zero in the  $A_1$  amplitude.

|  |   |  |                          |
|--|---|--|--------------------------|
| Good $A_1$ - $Z$ EXD                         | $\left  \frac{\text{Re}U_0}{\text{Im}U_0} \right  \gg 1$                | $\text{Re}U_0 < 0$   | $\text{Im}U_0 \approx 0$ |
| $A_1$ dominates over $Z$                     | $\left  \frac{\text{Re}U_0}{\text{Im}U_0} \right  < 1$                  | $\text{Re}U_0 > 0$   | $\text{Im}U_0 < 0$       |
| $Z$ dominates over $A_1$                     | $\left  \frac{\text{Re}U_0}{\text{Im}U_0} \right  > 1$                  | $\text{Re}U_0 < 0$   | $\text{Im}U < 0$         |
| Good $A_1$ - $Z$ EXD+ absorptive corrections | $\left  \frac{\text{Re}U_0}{\text{Im}U_0} \right  > 1$<br>For small $t$ | $\text{Re}U_0 < 0$<br>(But possibly changing sign for $t \approx -0.5$ ) | $\text{Im}U_0 \approx 0$ |

tion in low-energy potential models). We shall assume that the relative signs and magnitudes of the Reggeized  $0^{++}$ ,  $1^{--}$  exchange contributions are still given by the coupling properties of an elementary  $0^+$  exchange. This yields a prediction for  $N_0$  and  $N_2$  in terms of the empirically determined contribution to  $N_1$ .

Pole extrapolation is done in the usual way. Calculating with Feynman rules to obtain the amplitude near the pole, and then Reggeizing, one finds

$$\begin{aligned}\phi_1 &= \frac{g_{\epsilon pp}^2}{m_\epsilon^2 - t} 4m_N^2 \cos^2(\tfrac{1}{2}\theta_s), \\ \phi_5 &= \frac{g_{\epsilon pp}^2}{m_\epsilon^2 - t} 2m_N \sqrt{-t} (\cos \tfrac{1}{2}\theta_s) \\ \phi_2 &= \frac{g_{\epsilon pp}^2}{m_\epsilon^2 - t} t.\end{aligned}\quad (27)$$

Finally, the Regge coupling parameters [cf. Eq. (6)] are

$$\beta_{++}^\epsilon = -\beta_{+-}^\epsilon = 2m_N g_{\epsilon pp}.\quad (28)$$

After including the contribution of the exchange-degenerate partner of the  $0^{++}$ , one has a purely real ( $\epsilon, \omega'$ ) amplitude. The contribution to the real part of  $N_1$  is negative, as required to give a positive contribution to the polarization. The contribution to the real part of  $N_0$ , on the other hand, is positive.

The positive  $\epsilon$ - $\omega'$  contribution and the negative  $f$ - $\omega$  contribution in  $\text{Re}N_0$  cooperate to provide a relatively flat energy dependence of  $\rho = \text{Re}N_0/\text{Im}N_0$  over the range  $3 < p_{\text{lab}} < 10$  GeV/c. The values given in Table III,  $\beta_{++}^\epsilon = \beta_{+-}^\epsilon = 20$  have been adjusted to provide a reasonable fit to the  $I_t = 0$  component of the  $NN$  polarization (cf. Sec. IV). They are not too different from those inferred from potential-model analyses of low-energy  $NN$  scattering<sup>40</sup> which yield  $g_{\epsilon pp} = 13.3$ , and, therefore,

$$\beta_{++}^\epsilon = -\beta_{+-}^\epsilon \simeq 25.\quad (29)$$

Polarization in  $\pi N$  scattering also exhibits a rapidly varying ( $\sim s^{-0.5}$ )  $I_t = 0$  component.<sup>41</sup> Assuming that this effect is due to the same " $\epsilon$ " exchange that operates in  $NN$ , we deduce (via factorization) the estimate  $\beta_{\pi\pi^+\pi^-} \simeq 25$ . The decay width of the  $\epsilon(750)$  into  $\pi^+\pi^-$ , on the other hand, yields the much smaller value  $\beta_{\epsilon\pi^+\pi^-} \simeq 2.1$ . In Ref. 8, it is pointed out that  $\pi N$  data above 5 GeV/c show little evidence of an  $I_t = 0$  component. Of course it is difficult to detect a low-lying contribution [ $\alpha(0) \approx -0.5$ ] using only high-energy data. The authors of Ref. 8 limit themselves to high-energy data because of possible resonant effects in this nonexotic chan-

nel. However, a close study of the low-energy data<sup>41</sup> shows the  $I_t = 0$  effect to appear consistently in the 2–5 GeV/c range. Thus a Regge interpretation appears to be justified. We shall return to this issue in the conclusions.

#### IV. REGGE-POLE INTERPRETATION OF NUCLEON-NUCLEON DATA FOR SPIN OBSERVABLES

##### A. Amplitude components

In Fig. 1 we show Argand plots of our model amplitudes for  $pp$  scattering at 6 GeV/c laboratory momentum and both  $-t = 0.1$  and  $0.4$  GeV<sup>2</sup>. These plots are in substantial agreement with results of a preliminary amplitude analysis of the ZGS data.<sup>1</sup> We comment on each model component in turn.

##### 1. $N_0$

The magnitude of  $N_0$  is determined by that of the  $f$  (and  $\omega$ ) through  $f$  dominance of the Pomeron. Its sizeable real part is largely inherited from the EXD  $\omega + f$  contribution. At  $t = 0$  the magnitude and phase of  $N_0$  are measured at several energies. In the older data,  $\rho \equiv \text{Re}N_0/\text{Im}N_0 \approx -0.3$  at 6 GeV/c,<sup>42</sup> whereas in newer experiments  $\rho \approx -0.4$  is obtained.<sup>43</sup> In our model,  $\rho_{pp} = -0.43$  at 6 GeV/c. A further consequence of our simple  $f$  dominance of the Pomeron and EXD Regge-pole model is that  $\rho_{pp} \simeq 2\rho_{\pi^+\pi^-}$ , basically because the real part in  $pp$  scattering has contributions from  $\omega$  and  $f$  while that in  $\pi p$  has only an  $f$  contribution. At 6 GeV/c, the data<sup>42</sup> show  $\rho_{pp}/\rho_{\pi^+\pi^-} = 0.9 \pm 0.3$  rather than 2, suggesting that our model may predict too large a real part of  $N_0$  in  $pp$  scattering. The amplitude  $N_0$  is the dominant one in our model for all  $|t| \leq 1.0$  GeV<sup>2</sup>. It thus determines  $d\sigma/dt$  in magnitude and shape. Our differential cross section at 6 GeV/c is shown in Fig. 2; it is everywhere within 20% of the data. At 100 GeV/c, our model agrees very well with the experimental  $d\sigma/dt$ .<sup>7</sup> We remind the reader that our aim here is to present the expectations of the simplest Regge-pole model. Obviously more parameters could be introduced and a perfect "fit" obtained to the data in Fig. 2.

##### 2. $N_1$

According to Table III, the  $\omega + f$  and  $\rho + A_2$  contributions to  $N_1$  are about equal, although the former is not well determined since little is known about the precise strength of the isoscalar helicity-flip couplings to nucleons.<sup>21,22</sup> Accordingly, the Pomeron contribution to  $N_1$  is equally badly known. To help isolate the various contributions to  $N_1$  one can investigate the energy dependence of the elastic-scattering polarizations,  $P$ , for

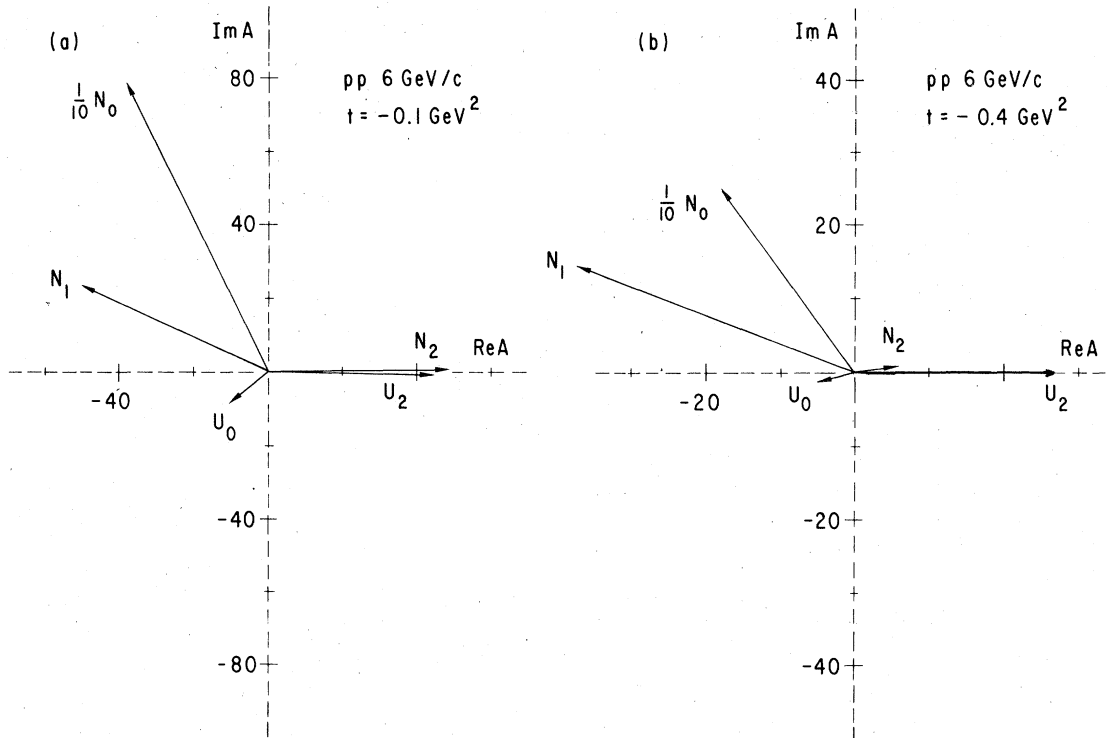


FIG. 1. Argand diagram showing the five  $pp$  amplitudes from our simple model at 6 GeV/c and (a)  $t = -0.1 \text{ GeV}^2$ , and (b)  $t = -0.4 \text{ GeV}^2$ .

$pp \rightarrow pp$  and  $pn \rightarrow pn$ . To a good approximation,<sup>8</sup> the  $I=1$  and  $I=0$  exchange components of  $N_1$  are given by

$$\begin{aligned} [P(pp) + P(pn)]^{\frac{1}{2}} [\sigma(pp)]^{1/2} &\approx -N_1^{I(0)}, \\ [P(pp) - P(pn)]^{\frac{1}{2}} [\sigma(pp)]^{1/2} &\approx -N_1^{I(1)}, \end{aligned} \quad (30)$$

where  $N_1^{I(t)}$  is the component of  $N_1$  orthogonal to  $N_0$  and having  $t$ -channel isospin  $I$ .

In the 2–12 GeV/c range,<sup>8</sup> the isospin-zero component is found to be very large ( $> |N_1^{I(1)}|$ ), but it falls with an effective trajectory  $\alpha_{\text{eff}}(t) \sim -0.5 + t$ . This has given rise to the suggestion that a low-lying Regge-pole corresponding to the scalar  $\epsilon$  (Ref. 39) or vector  $\omega'$  (Ref. 44) is contributing. In Sec. III B we obtained estimates of the sign and coupling structure of an EXD  $\epsilon$ ,  $\omega'$  Regge-pole contribution by pole extrapolation. The size of the  $\epsilon$  coupling is determined by potential model studies of low-energy nucleon-nucleon scattering.

$$\beta_{\epsilon}^{+-} = \beta_{\epsilon}^{++} \sim 20-25. \quad (31)$$

This is found (see Fig. 3) to give a good description of the  $I=0$  combination  $\frac{1}{2}[P(pp) + P(pn)]$  in the 3–12-GeV/c range, if we also use  $\alpha_{\epsilon}(t) = -0.5 + 0.9t$ . Note that in the absence of such a term,

the model can describe neither the rapid energy dependence nor the large magnitude of  $P$  at low energy. The scalar coupling structure is the most economical way of arranging a large contribution in  $N_1$ . (It also guarantees contributions to  $N_2$  and  $N_0$ . The contributions are positive both in  $N_2$  and in  $N_0$ . In  $N_0$ , the contribution serves to reduce  $|\rho_{pp}|$  at lower energies in agreement with the trend of the data.<sup>42</sup> In  $N_2$ , the positive  $\epsilon$  contribution helps in reproducing the behavior of  $C_{NN}$ .)

The fact that  $P(pn)$  data at 12 (Ref. 8) and 24 GeV/c (Ref. 45) become *negative* for  $|t| > 0.2 \text{ GeV}^2$ , and that  $P(pp)$  also tends to zero through *negative* values for  $|t| > 0.2 \text{ GeV}^2$  and  $45 \leq p_{\text{lab}} \leq 300 \text{ GeV/c}$  (Ref. 46), suggests<sup>47</sup> a high-energy (diffractive?) component in  $N_1^{I(0)}$ . The fact that  $P(pn)$  approaches asymptotic values earlier than  $P(pp)$  [ $P(pn)$  at 6 GeV/c  $\sim P(pp)$  at 45 GeV/c] may be partially explained by the cancellation of the competing  $I=0$  and  $I=1$  Reggeon-Pomeron interference terms in  $P(pn)$ .<sup>47</sup> Obviously, a pure pole Pomeron term cannot contribute to  $N_1^{I(0)}$  (which is orthogonal to  $N_0$ ). Somewhat arbitrarily, we set the real part of our flip Pomeron component to zero. This mimics the *relative*  $N_0, N_1$  phase expected in eikonal models with  $f$ -dominated Pomeron couplings,

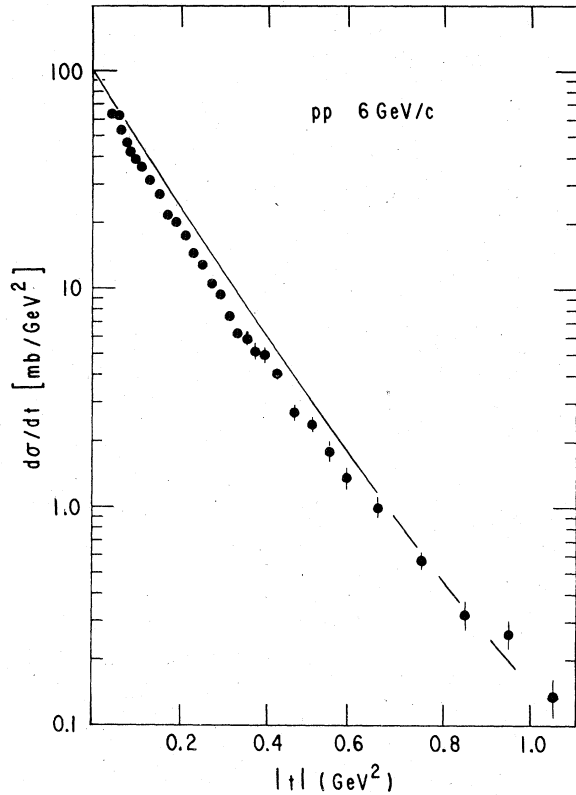


FIG. 2. Data on the 6-GeV/c  $pp$  differential cross section from Ref. 7 are compared with the expectations of the simple Regge-pole model described in the text.

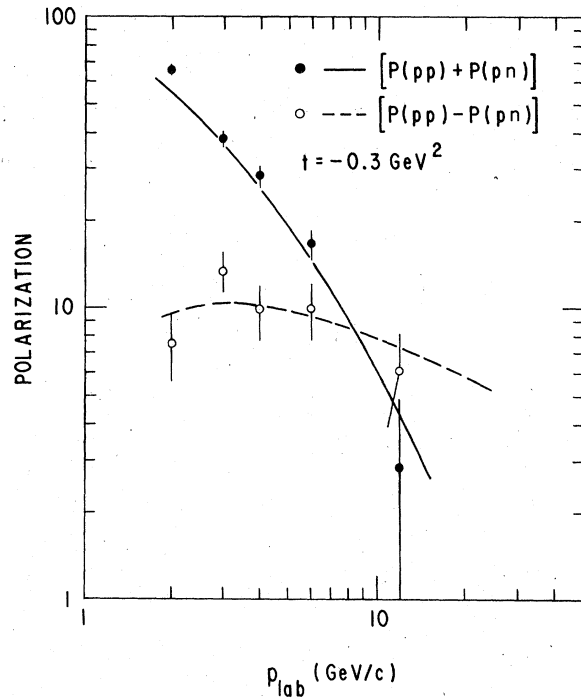


FIG. 3. Momentum dependence of the isospin  $I_t = 0$  and 1 components of the nucleon-nucleon polarization, Eqs. (30) of the text. Solid and dashed lines are from our model. Data are from Ref. 8.

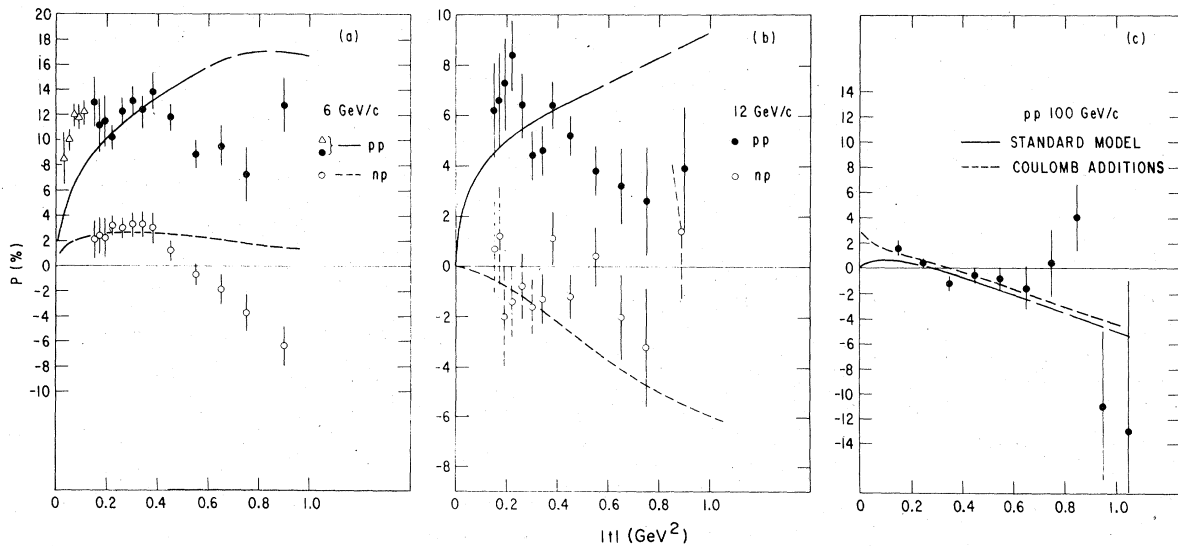


FIG. 4. Polarization data for  $pp$  and  $np$  elastic scattering, Refs. 8 and 9, are compared with the expectations of our simplest model at (a) 6 GeV/c and (b) 12 GeV/c. In (c) we show our model predictions (solid curve) at 100 GeV/c and the data from Ref. 46. The dashed curve in (c) provides our predictions when the Coulomb contributions are included, as described in Appendix C.

which Martin and Navelet have shown gives the correct sign.<sup>41(b)</sup> This allows a crude description of  $P(pp)$  and  $P(pn)$  at high energy (Fig. 4), at least for  $|t| \leq 0.6 \text{ GeV}^2$ , the region to which we limit our attention. (Improvements in the detailed description of the data are discussed below.)

All of our Regge poles come in exchange degenerate pairs. Thus all contributions to  $N_1$  are real, save for the Pomeron. The nonreal phase of  $N_1$  shown in Fig. 1 is due in our model to the significant contribution of the Pomeron.

### 3. $U_2$

This amplitude is expected to be dominantly  $I=1$  [i.e., that studied in  $np$  charge exchange (CEX)], and is described by the  $\pi+B$  and Williams "cut" contributions, as specified in Sec. III. It is also purely real in the model. According to the data<sup>19</sup>  $\Delta\sigma_T = -K' \text{Im}\phi_2 = 0.35 \pm 0.07 \text{ mb}$  at  $6 \text{ GeV}/c$ . From these data on  $\text{Im}\phi_2$ , together with our estimate of  $\text{Re}U_2 = (\frac{1}{2}\phi_2 \text{ at } t=0)$ , we deduce a phase of  $-3^\circ$  at  $6 \text{ GeV}$  and  $t=0$ . Our assertion that  $U_2$  is purely real is therefore a good approximation at small  $t$ . Models for the imaginary part of  $U_2$  at  $t=0$  are wholly dependent on the type of EXD breaking employed. Moreover,  $\text{Im}U_2$  at  $t=0$  is

described by a cut rather than a pole. Consequently we do not attempt to reproduce this rather minor feature of the data.

We note that our model describes  $C_{SS}$  adequately, Fig. 5(a), for  $|t| \leq 0.6 \text{ GeV}^2$  with our purely real  $U_2$ , in contrast to the standard strategy<sup>1,2</sup> which suggests that  $C_{SS}$  determines  $\text{Im}U_2$ .

### 4. $N_2$

This amplitude is dominated at small  $t$  by the same  $\pi+B$  cut which contributes to  $U_2$ . At large  $t$  it has important contributions from  $\rho+A_2$  exchange which couples strongly to helicity flip nucleon vertices. Isospin-zero exchanges, including the  $(\epsilon, \omega')$  and the Pomeron, are present but small. In the absence of contrary indications, we apply no absorptive corrections. A strong cancellation between the  $\pi+B$  cut and the  $\rho+A_2$  pole takes place at  $t \sim -0.3 \text{ GeV}^2$ , similar to that observed in  $K^*n \rightarrow K^*0p$ .<sup>31</sup> In the neighboring  $t$  interval,  $|N_2|$  is therefore small, perhaps too small, as can be seen in  $C_{NN}$ , which is sensitive to  $\text{Re}(N_0N_2^*)$  (see Fig. 6). The flip Pomeron contribution in our model provides  $N_2$  with a small positive imaginary part. We do not take this minor aspect of the model seriously since other effects which we do not

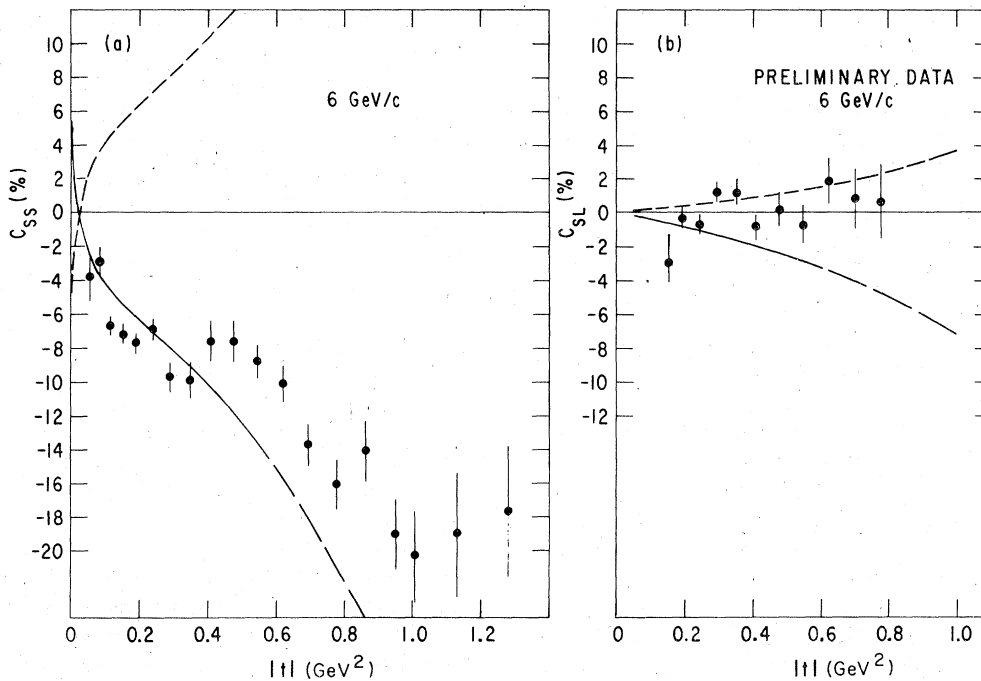


FIG. 5. Data on (a)  $C_{SS}$  (Ref. 14) and (b)  $C_{SL}$  (Ref. 15) for  $pp$  scattering at  $6 \text{ GeV}/c$ . The solid curves show our model expectations for  $pp$  scattering, and the short-dashed curves are our predictions for  $np$  elastic scattering.

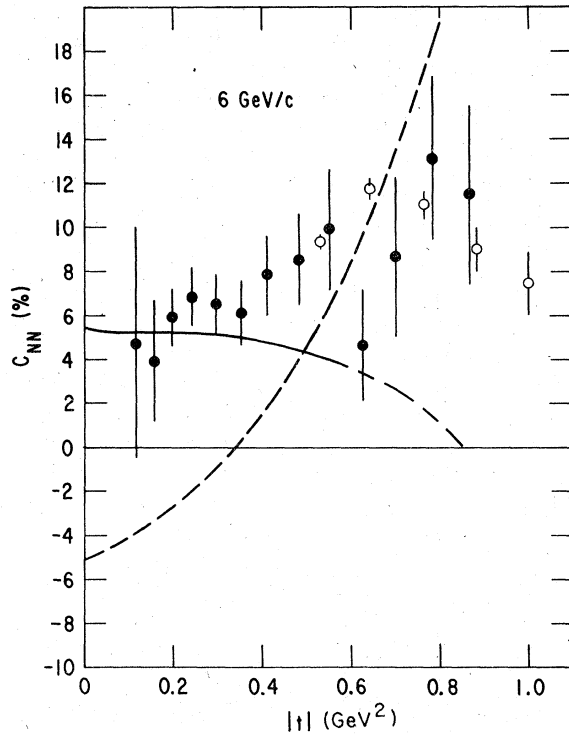


FIG. 6. Data from Refs. 11 and 12 on  $C_{NN}$  for  $pp$  scattering at 6 GeV/c are compared with the expectations of our simplest model. Our model expectations are shown as a solid curve for  $pp$  scattering and as a dashed curve for  $np$  elastic scattering.

try to incorporate (unitarity corrections, absorption, ...) may provide a compensating or larger negative imaginary part.

In the results of the preliminary amplitude analysis at  $t = -0.3 \text{ GeV}^2$ ,  $N_2$  is seen to lie in the fourth quadrant of the Argand diagram, close to the imaginary axis.<sup>1</sup> This result would appear to contradict naive expectations, based on strong exchange degeneracy, of a predominantly real  $N_2$ . However, as discussed above, the  $(\rho + A_2)$  and  $(\pi + B)$  cancellation reduces the real part substantially near  $t = -0.3 \text{ GeV}^2$ , leaving the imaginary part of  $N_2$ , from whatever source, with an abnormally large relative value at intermediate values of  $t$ . The negative value of  $\text{Im}N_2$  from the amplitude analysis also deserves a comment. It presumably arises from approximating  $C_{NN} \approx -\text{Im}N_0 \text{Im}N_2$ , on the assumption that  $N_0$  is dominant and purely imaginary. In our model, we are able to reproduce  $C_{NN}$  (and all other observables in the neighborhood of  $t = -0.3 \text{ GeV}^2$ ) with  $\text{Im}N_2 \geq 0$ . Thus our model may serve as an explicit counterexample to assumptions<sup>1</sup> built into the present amplitude analyses of  $pp$  scattering.

### 5. $U_0$

In our model, the Regge-pole ( $A_1 + Z$ ) contribution to  $U_0$  is real and negative (Sec. III A). According to the 6 GeV/c data for  $\Delta\sigma_L$ , a significant (EXD-breaking) imaginary part is present at  $t=0$ :

$$\text{Im}U_0/\text{Im}N_0 = \frac{1}{2} \Delta\sigma_L^L / \sigma_{\text{tot}}^L \approx -\frac{1}{70}. \quad (32)$$

Since  $\text{Im}U_0$  is comparable to our pole-extrapolation estimate of  $\text{Re}U_0$ , we must parametrize its effect in order to have a realistic model. We use

$$\text{Im}U_0 = -26e^{4t}(\alpha's)^{\alpha_{A_1}}, \quad (33)$$

where the  $t$  dependence is *a priori* unknown but has a strong influence on the parameter  $C_{LL}$  (shown in Fig. 7). Away from  $t=0$ , the dominant contribution is from

$$C_{LL} \propto -\text{Re}N_0 \text{Re}U_0 - \text{Im}N_0 \text{Im}U_0. \quad (34)$$

The first term is always negative, but at small  $t$ ,  $-\text{Im}N_0 \text{Im}U_0$  is known to be large and positive (from  $\sigma_{\text{tot}}$  and  $\Delta\sigma_L^L$ ), so that  $C_{LL}$  is also positive [see Fig. 7(a)]. Provided  $\text{Im}U_0$  falls reasonably fast with  $t$  [e.g., Eq. (33)]  $C_{LL}$  changes sign as  $\text{Re}N_0 \text{Re}U_0$  begins to dominate.

Since  $U_0$  has definite exchange naturality only to leading order in  $1/s$ , one may wonder whether the large value of  $\text{Im}U_0$  is a nonasymptotic "contamination." In Appendix A we explore this question in some detail, showing, in particular, that  $U_0$  receives a nonasymptotic contribution from  $N_0$ , having the form  $U_0 = -(t/2s)N_0^P$ . Here  $N_0^P$  is the Pomeron part of  $N_0$ . Because  $N_0^P$  is relatively large, this effect is non-negligible. However, because  $N_0^P$  is also primarily imaginary, the correction to  $U_0$  is essentially just a redefinition of the theoretically unspecified nature of  $\text{Im}N_0$ . Adding this correction to our basic  $U_0$ , we obtain the results for  $C_{LL}(t)$  shown in Fig. 7(b).

Our expression for  $\text{Im}U_0$ , with the value  $\alpha_{A_1}(0) = -0.19$  determined in Sec. III A, provides a fine representation of  $\Delta\sigma_L$  for  $p_{\text{lab}} \geq 3 \text{ GeV}/c$  (Fig. 8). We predict  $\Delta\sigma_L = -0.5 \text{ mb}$  at 12 GeV/c, and  $-0.04 \text{ mb}$  at 100 GeV/c. Below 3 GeV/c,  $\Delta\sigma_L$  displays rapid energy dependence, which has led to speculation that one or more isolated resonances may be present in the  $pp$  system between  $p_{\text{lab}} = 1$  and 3 GeV/c.<sup>23</sup> Whatever the physical origin of the large and rapidly varying behavior of  $\text{Im}U_0$  below 3 GeV/c, it is not embodied in our model, and we restrict our attention to higher energies.

Note that the signs of all the Regge-pole contributions are determined by our pole-extrapolation procedure [Eq. (6)] and are in agreement with the data in the cases where they may be checked ( $f, \omega, \pi + B, \rho + A_2$ ). Our magnitudes and phases shown in Fig. 1 agree reasonably well with the

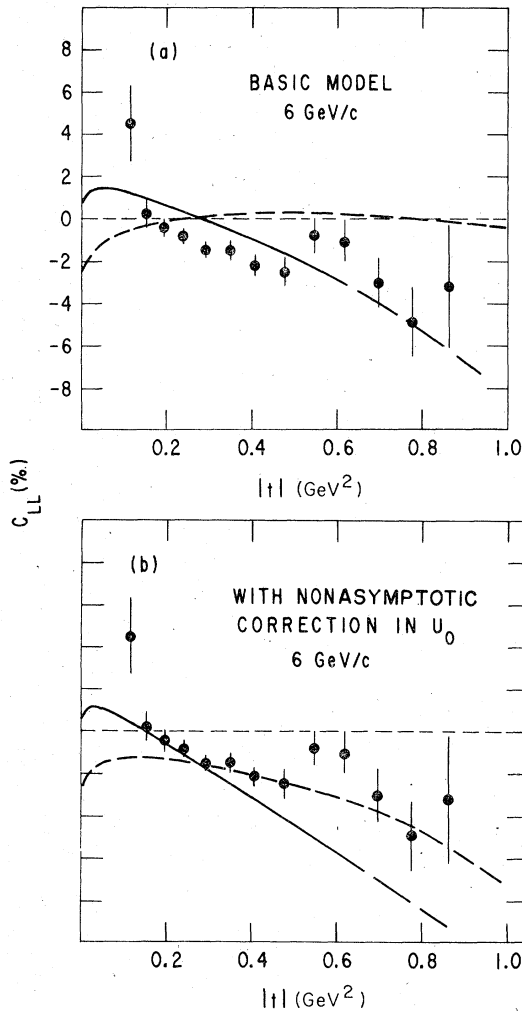


FIG. 7. Data on  $C_{LL}$  (Ref. 13) for  $pp$  scattering at 6 GeV/c. In (a) we present the predictions of our simplest model for both  $pp$  (solid curve) and  $np$  (short-dashed curve) elastic scattering. In (b) we show the results we obtain after including in  $U_0$  the nonasymptotic Pomeron correction discussed in the text and in Appendix A.

results of preliminary amplitude analyses of  $pp$  data. It will be very surprising if the final amplitude analyses prove the phases shown in Fig. 1 to be wrong by more than  $30^\circ$  in each case.

## B. Predictions for further observables

### 1. $pp$ scattering at 6 GeV/c.

The model amplitudes outlined above in Sec. IV A have been fixed without reference to  $pp$  scattering data save in the following respects:

- (a) the phase of the helicity flip Pomeron from  $[P(pp)]$ ,
- (b) the EXD-violating contributions to  $\text{Im}U_0(A_1$

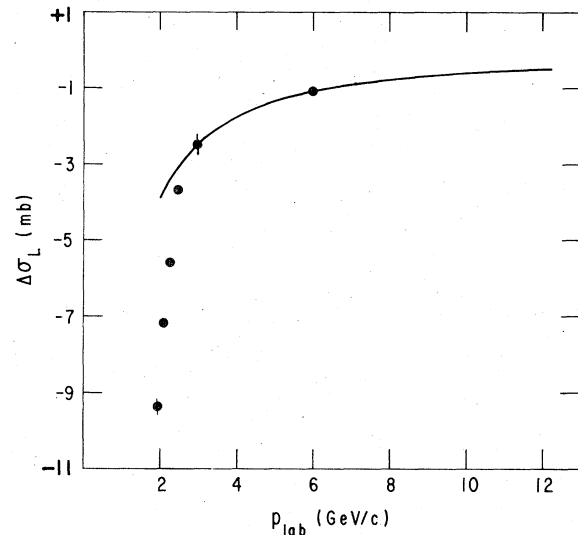


FIG. 8. Our expectation for  $\Delta\sigma_L$  in  $pp$  scattering is plotted versus lab momentum. The data are from Refs. 13 and 20.

+Z). We compare our predictions with data on  $C$ -type observables in Figs. 5, 6, and 7. In Figs. 9, 10, and 11, we present our predictions for  $D$ -type,  $K$ -type, and  $H$ -type observables. All predictions of the model are in reasonable agreement with the available 6 GeV/c data for  $pp$  spin observables. Preliminary data<sup>1</sup> also suggests  $K_{SS} = (3 \pm 10)\%$  in agreement with our predictions.

Because the magnitudes of the various exchanges are taken from analyses of data other than  $pp$ , and because phases and  $t$  dependences are fixed by theoretical considerations, we believe that the general success of our description of all spin observables at 6 GeV/c in the range  $|t| \lesssim 0.6 \text{ GeV}^2$  is a nontrivial verification of our simple Regge-pole approach. All quantities expected to be small are small; all predicted to be large are large; the signs are correct. Data on  $H_{LSN}$  will be important for confirming the size of our  $A_1$ -type exchange. Our worst failures are in our naive representation of  $P$ , Fig. 4,  $C_{NN}$ , Fig. 6, and  $K_{NN}$ , Fig. 10(a). These defects can be remedied by modest modification of the QUADREM package<sup>22</sup> together with the introduction of small EXD-breaking effects. Difficulties with  $C_{NN}$  and  $K_{NN}$  are greatly alleviated if a small negative imaginary part is introduced in  $N_2$ . This must be interpreted as an EXD-breaking effect. It has the property of preventing the vanishing of  $\text{Re}(N_0 N_2^*)$  in the neighborhood of  $|t| \approx 0.4 \text{ (GeV/c)}^2$ . Since  $C_{NN}$  at  $p_{\text{lab}} = 12 \text{ GeV/c}$  (Ref. 12) remains positive for  $|t| \gtrsim 0.6 \text{ (GeV)}^2$ , the EXD-breaking effect is required to have fairly slow energy dependence. Thus a cut associated with the  $\rho, A_2$  term may be

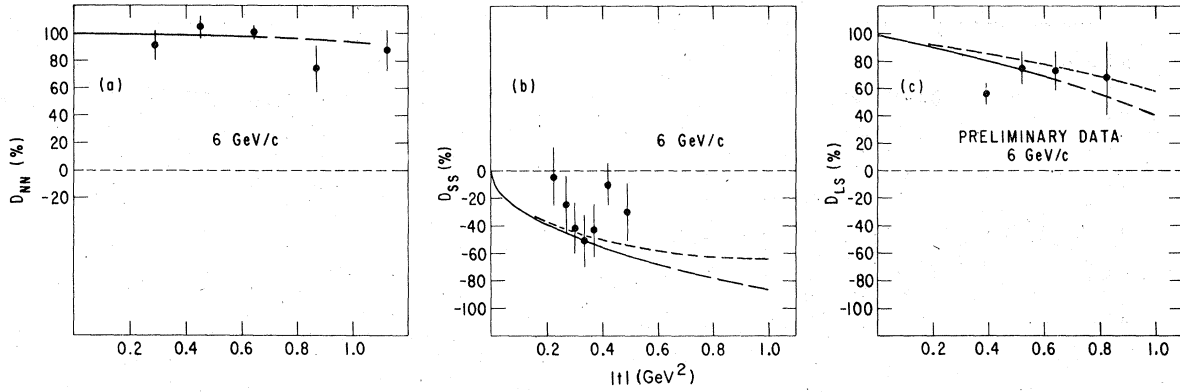


FIG. 9. (a) Data from Ref. 17 on  $D_{NN}$  in  $pp$  scattering at 6 GeV/c are compared with our expectations. In our model, the  $D_{NN}$  predictions for  $pp$  and  $np$  elastic scattering are essentially identical. (b) Data from Ref. 18 on  $D_{SS}(R)$  for  $pp$  scattering at 6 GeV/c are compared with our model expectations (solid line). Also shown is our prediction for  $np$  scattering (short-dashed line). (c) Data from Ref. 1 on  $D_{LS}$  for  $pp$  scattering at 6 GeV/c and our model expectations for both  $pp$  and  $np$  elastic scattering.

more appropriate than a  $\pi, B$  cut. The results of our improved model for  $C_{NN}$  and  $K_{NN}$  are shown in Fig. 12.

Our discrepancies in describing  $P$  in Fig. 4 fall into three classes. First, we fail to reproduce the  $t$  dependence, especially for  $|t| > 0.3$  GeV<sup>2</sup>. We achieve too little polarization in  $pp$  scattering at small  $t$ . Finally, the change of sign of the  $np$  polarization at 6 GeV/c is not reproduced. The  $t$  dependence at large  $t$  is remedied easily by introducing a small additional exponential damping of the Regge propagators. To achieve the change in sign of  $np$  polarization, it is sufficient that this added damping be slightly greater for the  $I_t = 0$  exchange components.<sup>41(b)</sup> Lastly, to augment  $P(pp)$  at small  $t$ , we reduce our estimate of the size of the Pomeron flip term, and we increase the values of various Regge coupling by  $\sim 10\%$ . Thus, rather than  $x_p = 1$  in Eq. (11), a better choice for  $N_1$  is  $x_p = 0.3 \exp(-1.1t)$ . A reduced flip coupling is also consistent with results of analyses of the Pomeron flip coupling to mesons.<sup>27</sup> We list below the modifications of our basic model that yield the curves in Figs. 12 and 13.

$$\begin{aligned}
 (\beta_{pp}^e)_{++} &= -\beta_{pp}^e : 20 - 24e^{0.7t}, \\
 (\beta_{pp}^f)_{+-} &: 1.9 - 1.9e^{1.4t}, \\
 (\beta_{pp}^p)_{++} &: 1.63 - 1.96e^{0.4t}, \\
 (\beta_{pp}^p)_{+-} &: 13 - 14.3e^{0.4t}, \\
 (\beta_{pp}^p)_{+-} &: 1.9 - 0.57e^{-1.1t}, \\
 \text{Im}N_2 &: 0 - 16.3t(0.9s)^{0.5} e^{(1.65+b)t},
 \end{aligned} \tag{35}$$

$$b = \frac{[3.1 + 0.3 \ln(0.9s)][1 + 0.9 \ln(0.9s)]}{[4.1 + 1.2 \ln(0.9s)]}.$$

In parametrizing  $\text{Im}N_2$  we have in mind a ( $\rho, A_2$ )

$\otimes P$  cut effect. This is expected to have a very small imaginary part at  $t=0$ , and a "shrinking"  $t$  dependence similar to that expressed above. Note that the above parametrization implies a very small departure from the expectation that the contribution of  $\rho, A_2$  to  $N_2$  is real. For  $p_{1ab} = 6$  GeV/c and  $|t| = 0.5$  GeV<sup>2</sup>, one finds

$$\text{Im}N_2 / \text{Re}N_2^{p, A_2} \approx 0.15 \tag{36}$$

We note that our improved model provides an excellent representation of the polarization data. The improvements require only very modest changes from our simplest model.

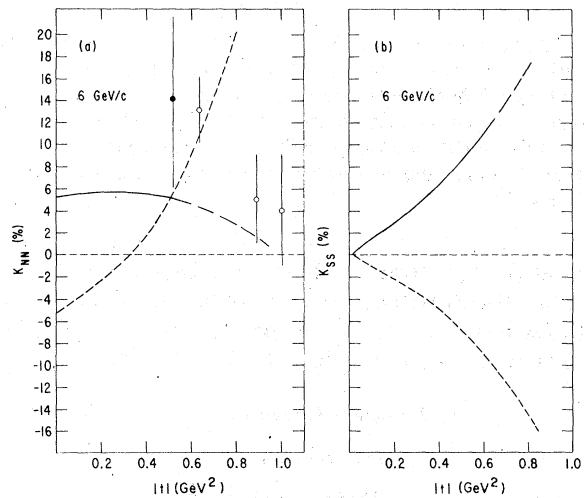


FIG. 10. (a)  $K_{NN}$  at 6 GeV/c. The data are from Ref. 16. Our expectations for  $pp$  are shown as a solid line and for  $np$  elastic scattering as a short-dashed line. (b) Our predictions for  $K_{SS}$  at 6 GeV/c for  $pp$  and  $np$  elastic scattering.

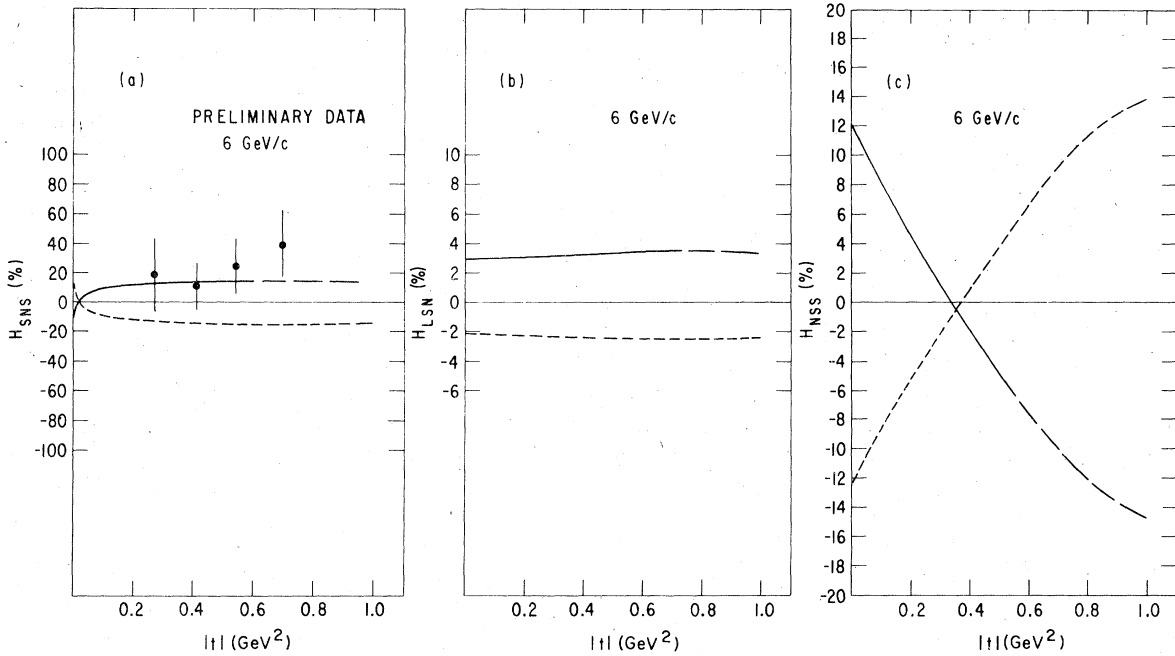


FIG. 11. (a) The observable  $H_{SNS}$  at 6 GeV/c. The  $pp$  data are from Ref. 1. Our predictions for (a)  $H_{SNS}$ , (b)  $H_{LSN}$ , and (c)  $H_{NSS}$  are shown as solid curves for  $pp$  scattering and as short-dashed curves for  $np$  elastic scattering.

2.  $np \rightarrow np$  at 6 GeV/c.

Spin-correlation measurements for  $pn \rightarrow pn$  are also envisaged. These will provide useful information on the isospin decomposition of amplitudes in those cases where a significant part of the bi-

linear product comes from an  $I=0, I=1$  interference. This is true for  $\Delta\sigma_{tot}^L$ ,  $C_{NN}$ ,  $C_{LL}$ ,  $C_{SS}$ ,  $K_{NN}$ ,  $K_{SS}$ ,  $H_{SNS}$ ,  $H_{NSS}$ , and  $H_{LSN}$ . Predictions for  $np$  elastic scattering at 6 GeV/c are shown as short-dashed curves in Figs. 4-7 and 9-11. The mirror symmetry of  $C_{SS}$  between  $pp$  and  $np$  is

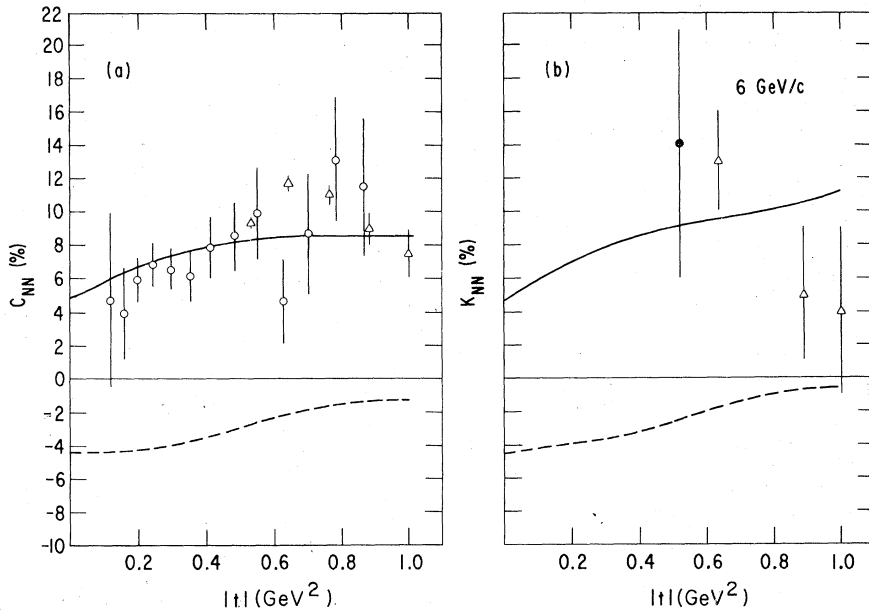


FIG. 12. Results of our improved model are compared with (a) the 6-GeV/c  $pp$  data on  $C_{NN}$  from Refs. 11 and 12 and with (b) the data on  $K_{NN}$  from Ref. 16.

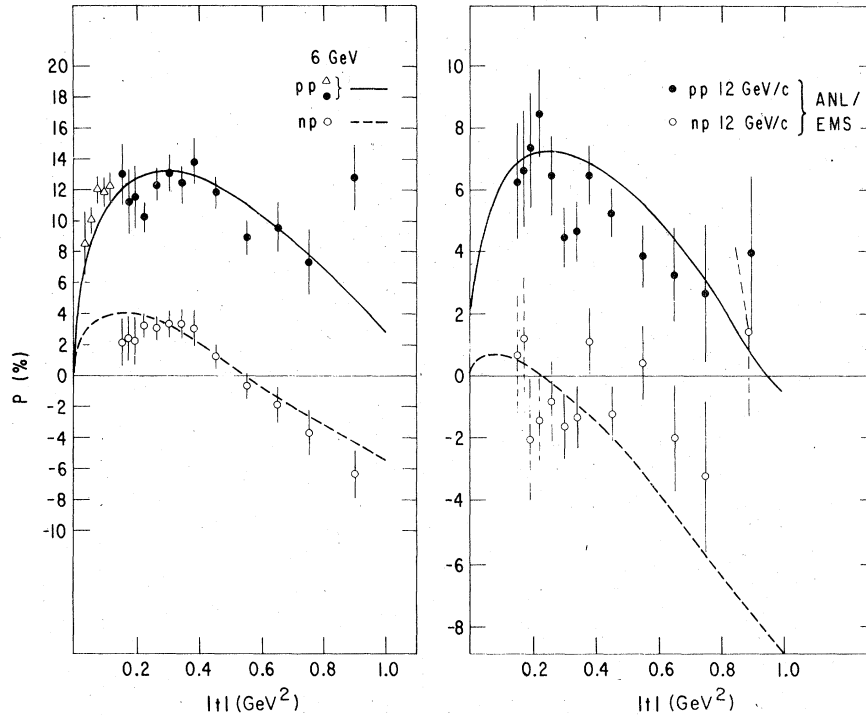


FIG. 13. Results are shown from our improved model: (a) 6 GeV/c, and (b) 12 GeV/c polarization for  $pp$  and  $np$  elastic scattering.

“guaranteed” by the dominance of  $N_0$ . Lack of such in the data might suggest the presence of contributions with the quantum numbers of  $(\eta, H)$  in  $U_2$ . Measurements of  $C_{NN}$  for  $np$  elastic would help to establish the isospin structure of  $N_2$ , separating the roles of the  $(\rho, A_2)$  and  $(\epsilon, \omega')$  contributions. The  $D$ -type quantities for  $np$  elastic do not seem to us especially interesting. Data on  $K_{NN}$  and  $K_{SS}$  would be useful as adjuncts to  $C_{NN}$  and  $C_{SS}$ , respectively. Information on  $H_{LSN}$  would establish the isospin of  $\text{Re}U_0$ , which is dominantly  $I_t=1$  in our model. Finally, measurement of  $\Delta\sigma_L(np)$  establishes the isospin of  $\text{Im}U_0$  which we have entirely arbitrarily chosen to be an  $I_t=1$  effect in our model.

In a limited program of  $np$  elastic spin measurements at 6 GeV/c, we suggest  $\Delta\sigma_L$ ,  $C_{NN}$ ,  $C_{SS}$ , and  $H_{LSN}$  as “best buys.”

### 3. $np$ charge exchange at 6 GeV/c

Of particular value to the phenomenologist would be spin-correlation measurements of  $np$  charge exchange. The  $t$ -channel isospin is unique, eliminating all  $I_t=0$  exchanges, including the notorious Pomeron. Present in  $np$  CEX are the reasonably well constrained  $(\rho, A_2)$  and  $(\pi, B)$  exchanges, as well as the “new”  $(A_1, Z)$  pair. With a polarized deuteron beam or a polarized deuteron target,  $C_{xx}$

type measurements are feasible and valuable. The asymmetries expected for  $C_{LL}$  and  $C_{SL}$  are particularly large in our highly simplified model, as we show in Fig. 14(a); e.g.,  $C_{LL} \sim 80\%$  at  $|t| \approx 0.1$  GeV<sup>2</sup>.  $C_{LL} [\propto \text{Re}N_2 U_2^*]$  is sensitive to the pole-cut cancellation effects in  $N_2$ .  $C_{SL} (\propto \text{Re}U_2 N_1^*)$  should help determine the properties of  $N_1$  and the “true” origin of simple polarization  $P$  (is there a non-real phase in  $N_2$  or  $N_1$  or both?). In experiments with a polarized proton beam and polarized deuteron target, any of the  $D$ -type or  $K$ -type quantities would be useful. As shown in Figs. 14(b) and 14(c), we again expect large values,  $\sim 50\%$ .  $D_{NN}$  for  $np$  CEX is particularly valuable for model builders in that it separates the magnitudes of natural- and unnatural-parity exchanges. Since we have not varied parameters in an attempt to optimize a fit to existing  $np$  CEX data, our predictions in Fig. 14 should not be regarded as the best we could achieve. Rather we present them as typical of the large magnitudes expected for spin-correlation observables in CEX, as opposed to elastic scattering. Data on some of these observables would be a valuable stimulus for further phenomenological work.

### 4. Higher energies

Present data on  $pp$  spin observables at 12 GeV/c are limited to  $P$ , over a fairly wide range of  $t$ ,

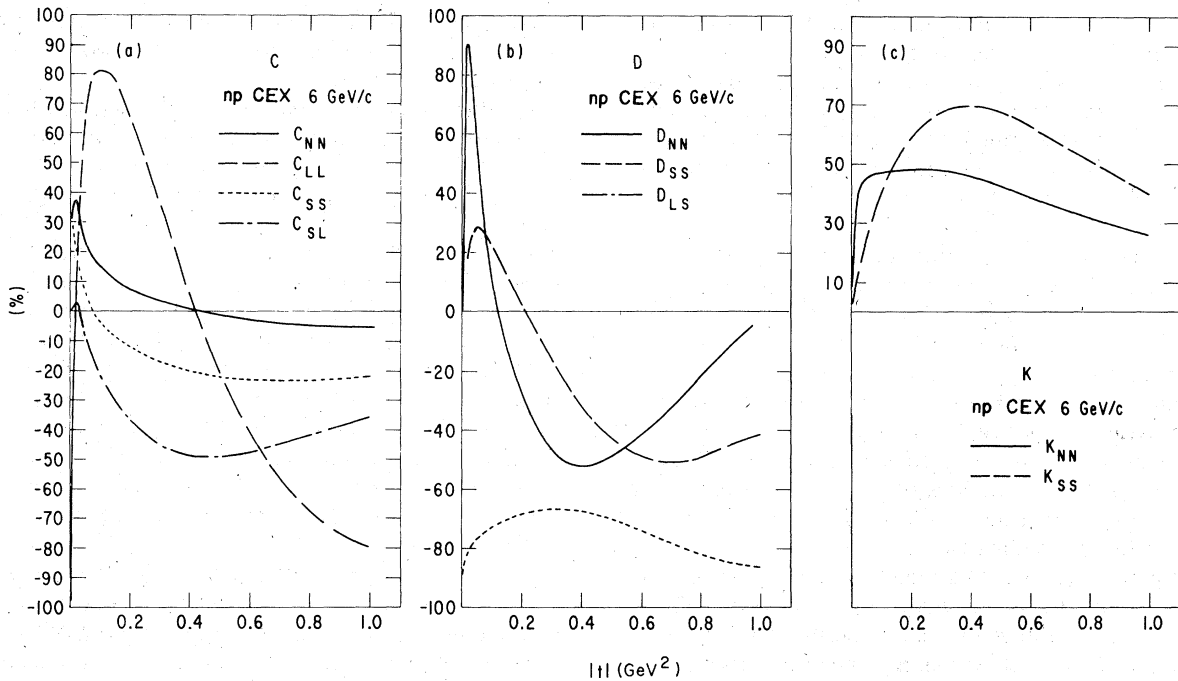


FIG. 14. Our predictions for spin observables in  $np$  charge exchange at  $6 \text{ GeV}/c$ : (a)  $C$ -type; (b)  $D$ -type; and (c)  $K$ -type observables.

and  $C_{NN}$  for  $|t| > 0.5 \text{ GeV}^2$ . Owing to the limited projected lifetime of the ZGS, we do not foresee the possibility of a complete program of spin measurements at  $12 \text{ GeV}/c$ . The importance of such a program is tied to the value one attributes to separating, via their different energy dependences, the effects of exchanges with intercepts  $\alpha(0) \sim \frac{1}{2}(\rho, f, \omega, A_2)$  from those with  $\alpha(0) \leq 0(\pi, B, A_1, Z, \dots)$ . This use of  $12 \text{ GeV}/c$  data is illustrated by the analysis of the  $12 \text{ GeV}/c$  data on  $P(pp)$  and  $P(pn)$ .<sup>8</sup> A measurement of  $\Delta\sigma_L$  for  $pp$  scattering at  $12 \text{ GeV}/c$  is imperative. It will illuminate the origin of the  $A_1$ -like components (energy dependence of  $\Delta\sigma_{\text{tot}}^L$ ). In our model, most spin correlation terms are very close to 0 or 1 at this energy, and consequently contain little information. Measurable values are expected, however, for  $D_{SS}$  ( $\sim -30\%$  at  $|t| \sim 0.2 \text{ GeV}^2$ ) and  $H_{SNS}$  ( $6\%$ ).  $C_{LL}$  is expected to be less than  $1\%$ . We do not provide curves of our  $12\text{-GeV}/c$  predictions in this paper but would be glad to supply them to interested readers.

##### 5. Low-energy extrapolation

All measurables investigated experimentally display rapid variation with energy for  $p_{1\text{ab}} \lesssim 3 \text{ GeV}/c$ :  $\rho$ ,  $\Delta\sigma_L$ ,  $\Delta\sigma_T$ ,  $P$ ,  $C_{NN}$ , and  $C_{LL}$ . Above  $3 \text{ GeV}/c$ , the rapid decrease with energy of the  $I_t=0$  component of  $P$  has led to conclusions that a

natural-parity  $I_t=0$  exchange with  $\alpha(0) \approx -0.5$  is strongly coupled to nucleons. Below  $3 \text{ GeV}/c$ , the energy dependence of  $P$  was exploited to help pin down the parameters of a possible dibaryon resonance.<sup>23</sup> As shown in Fig. 8, our model adequately describes the energy dependence of  $\Delta\sigma_L$  for  $p_{1\text{ab}} \geq 3 \text{ GeV}/c$ , in terms of an unnatural-parity  $A_1$ -type exchange, but it is obviously inadequate for  $\Delta\sigma_L$  below  $3 \text{ GeV}/c$ . We are also unable to interpret the large value of  $\Delta\sigma_T$  for  $p_{1\text{ab}} \leq 2.5 \text{ GeV}/c$ . Stated otherwise, our model does not include a mechanism for generating large imaginary parts, which change rapidly with energy in  $\phi_2$  and in  $(\phi_1 - \phi_3)$ . Unless these are included, it is fruitless to attempt a fit to  $pp$  data for  $p_{1\text{ab}} \lesssim 3 \text{ GeV}/c$ . In particular, a proper description of  $C_{NN}$  requires specification of the product  $\text{Im}U_0 \text{Im}U_2$ . In the data this term is large and positive at  $t=0$  and  $p_{1\text{ab}} \lesssim 3 \text{ GeV}/c$ , but is zero in our model. At best, our model could serve as a "background" at these low momenta, permitting the identification of rapidly varying components via a subtraction procedure. However, the customary caution must be voiced regarding Regge models at low momenta.

##### V. CONCLUSIONS

Current knowledge of Reggeon couplings to nucleons is sufficiently good that we can confidently predict the helicity structure and the relative

sizes of the various exchanges in  $NN$  elastic scattering. Since our knowledge of unitarity effects (absorption systematics) is not quite on the same footing, the phases of the amplitudes are not predictable with as much assurance. It is for this reason that we stress the measurement of observables which determine the real parts of amplitudes.

In elastic  $pp$  scattering, the "upper" and "lower" vertices of our exchange diagrams are identical. This allows a powerful test of pole-extrapolation concepts and of Regge parameters, since the couplings enter squared. The richness of the exchange structure in  $pp$  scattering permits an examination on an equal footing of many different exchange phenomena (Pomeron,  $\pi$ , natural- and unnatural-parity exchanges, scalar exchange, both isospins, ...). Otherwise this information must be culled from disparate sources.

We have presented a model which embodies our best knowledge of the couplings, which describes the major features of the available polarization data, and which provides a convenient standard of comparison for the forthcoming amplitude analyses of  $pp$  scattering. Its usefulness as a template derives from its theoretical simplicity—EXD Regge poles, SU(3) symmetry,  $f$ -dominated Pomeron, and simple absorption for  $\pi$  exchange. Each coupling has a sensible value at the position of the exchange pole.

Relatively new information extracted from the  $pp$  spin-correlation data includes the role of low-lying unnatural-parity (axial-vector)  $A_1$ -type exchanges and confirmation of a strongly coupled low-lying natural-parity  $I=0$  ( $\epsilon$ ,  $\omega'$ ) exchange.<sup>39,44</sup> The size of the hadronic axial-vector term in  $pp$  scattering is consistent with our theoretical estimates. This conclusion rests on our description of  $C_{LL}(t)$  and needs confirmation from data on  $H_{LSN}$ . Identification of the  $A_1, Z$  type of exchange in  $pp$  scattering with the expected magnitude complements recent achievements in spectroscopy in which the  $A_1$  resonance seems finally to have been identified.<sup>30</sup>

The sizeable  $I_t=0$  low-lying ( $\epsilon$ ,  $\omega'$ ) exchange in  $N_0, N_1$ , and  $N_2$  deserves a comment. A low-lying exchange was first observed to be necessary in order to describe the energy dependence of the polarization.<sup>9</sup> The assumption that it corresponds to a factorizable singularity<sup>39</sup> implies that it will be present not only in  $N_1$  but also in  $N_0$  and  $N_2$ . We choose to identify it as an  $\epsilon$ -type exchange because its size in  $N_0$  and  $N_2$  is consistent with pole-extrapolation estimates of a scalar exchange term. It is especially gratifying that the presence of such an exchange contribution in  $N_2$  is necessary to understand the  $t$  dependence of  $C_{NN}$ . The rapid

energy variation of the same parameter between 4 and 6 GeV/ $c$  is also partially accounted for by the ( $\epsilon$ ,  $\omega'$ ) contribution.

Whether such an exchange could be associated with baryonium states<sup>48</sup> is an open question since so little is known about the properties of such states except perhaps their probable intercepts. However, it is curious that a similarly large low-lying effect is discernable in  $\pi N$  scattering.<sup>41</sup> The effect in  $\pi N$  is too large when compared with the "known"  $\epsilon$  coupling strength to  $\pi\pi$  and obviously should not be connected with baryonium effects.

Most expectations of our simplified model are supported, as discussed in Sec. IV, but the data do provide evidence for interesting deviations:

(a) The real/imaginary ratio of the dominant amplitude,  $N_0$ , at  $t=0$  is perhaps smaller than indicated by  $f$  dominance of the Pomeron and EXD  $\omega+f$  exchange.

(b) At  $t=0$ , a large (EXD-violating) contribution to  $A_1+Z$  exchange is present in  $U_0$ . More information on its energy dependence ( $\Delta\sigma_{tot}^Z$ ) will be required to establish the true origin of this effect.

(c) Either the magnitude of the spin-flip Pomeron contribution or the Pomeron phase (or both) are poorly understood. This is suggested in part by our difficulties in achieving a wholly satisfactory representation of the  $t$  dependence of  $P$  with our simplest model.

Above 10 GeV/ $c$ , few spin-correlation measurements are expected to have sizable values at small  $t$ . In Sec. IV, we have listed those that do. On the other hand, as also described in Sec. IV, spin-correlation measurements of  $np$  CEX and  $np$  elastic scattering at 6 GeV/ $c$  are expected to give significant results and are essential for further phenomenological progress.

#### ACKNOWLEDGMENTS

One of us (A.C.I.) is grateful for the kind hospitality of the High Energy Physics Division at Argonne National Laboratory where much of this work was done. We are indebted to Aki Yokosawa, Hal Spinka, and other members of the High Energy Physics Division Polarization Group for generous access to their data and for informative discussions. We have also benefited from conversations with G. H. Thomas. This research was performed under the auspices of the United States Department of Energy.

#### APPENDIX A: NONLEADING CONTRIBUTIONS FROM NATURAL-PARITY EXCHANGES

In the preceding sections, we discussed at some length the low-lying  $\epsilon$  and  $A_1$  Regge-pole contri-

butions which are only apparent at low energies. Since the amplitudes  $N_0$ ,  $N_1$ ,  $N_2$ ,  $U_0$ , and  $U_2$  have definite exchange naturality only to leading order in  $1/s$  one might reasonably question the identification of these exchanges. For example, data suggest  $\text{Im}U_0/\text{Im}N_0 \approx -\frac{1}{70}$  at 6 GeV/c and  $t=0$  compared with  $1/s \approx 1/13$ —i.e., our “ $A_1$ ”-exchange term is potentially some 5 times smaller than a

typical nonleading Pomeron contribution. Furthermore, the  $A_1$  and nonleading Pomeron would have similar energy dependences. A proper interpretation of the amplitude structure thus requires a study of these nonasymptotic contributions of the wrong naturality. We turn now to this question.

For ease of reference we reproduce the helicity crossing relations<sup>49</sup>

$$\begin{aligned} N_0 &= \frac{1}{2}(\phi_1^s + \phi_3^s) = \frac{1}{2}[\sin^2\chi(\phi_1^t + \phi_2^t) - \cos^2\chi(\phi_3^t - \phi_4^t) - 4\sin\chi\cos\chi\phi_5^t], \\ N_1 &= \phi_5^s = -\frac{1}{2}\sin\chi\cos\chi[(\phi_1^t + \phi_2^t) + (\phi_3^t - \phi_4^t)] + (\cos^2\chi - \sin^2\chi)\phi_5^t, \\ N_2 &= \frac{1}{2}(\phi_4^s - \phi_2^s) = \frac{1}{2}[\cos^2\chi(\phi_1^t + \phi_2^t) - \sin^2\chi(\phi_3^t - \phi_4^t) + 4\sin\chi\cos\chi\phi_5^t], \\ U_0 &= \frac{1}{2}(\phi_1^s - \phi_3^s) = \frac{1}{2}(\phi_3^t + \phi_4^t), \quad U_2 = \frac{1}{2}(\phi_2^s + \phi_4^s) = \frac{1}{2}(\phi_1^t - \phi_2^t), \end{aligned} \quad (\text{A1})$$

with

$$\cos\chi = \left[ \frac{st}{(s-4m^2)(t-4m^2)} \right]^{1/2}, \quad \sin\chi = \left[ \frac{4m^2u}{(s-4m^2)(t-4m^2)} \right]^{1/2}. \quad (\text{A2})$$

The superscripts  $s$  and  $t$  distinguish  $s$ - and  $t$ -channel helicity amplitudes.

Approximately parity-conserving helicity amplitudes are defined in terms of (exactly parity-conserving)  $t$ -channel partial-wave amplitudes  $\phi_i^{tJ\pm}$  by

$$\hat{\phi}_i^{t\pm} = \sum_{J=M}^{\infty} (2J+1) [e_{\lambda\mu}^{J+}(z_t)\phi_i^{tJ\pm} + e_{\lambda\mu}^{J-}(z_t)\phi_i^{tJ\mp}], \quad (\text{A3})$$

where  $\lambda = \lambda_a - \lambda_b$ ,  $\mu = \lambda_c - \lambda_d$ ,  $M = \max\{|\lambda|, |\mu|\}$ , and the  $e_{\lambda\mu}^{J\pm}(z_t)$  are the appropriate combinations of  $d$  functions introduced by Gell-Mann *et al.*<sup>50</sup> They have the property that

$$e_{\lambda\mu}^{J\pm}(z_t) = 0, \quad \text{if } |\lambda| \text{ or } |\mu| = 0. \quad (\text{A4})$$

Thus  $t$ -channel amplitudes which have zero helicity flip at at least one vertex (i.e.,  $\phi_1^t, \phi_2^t, \phi_5^t$ ) give rise to “parity-conserving” amplitudes Eq. (A3) which are *exactly* parity conserving to all orders in  $1/s$ . Thus,  $(\phi_1^t + \phi_2^t)$  and  $\phi_5^t$  correspond exactly to natural-parity exchange, whereas  $(\phi_3^t - \phi_4^t)$  corresponds to unnatural-parity exchange. A first conclusion from the crossing relations is, therefore, that the amplitude  $U_2$  is uncontaminated by natural-parity effects to all orders in  $1/s$ .

Discussion of  $U_0$  requires a few more steps. The contribution of a natural-parity trajectory  $\alpha$  to the various amplitudes is

$$\begin{aligned} \phi_1^t + \phi_2^t &= \gamma_{++}^{-2} (\alpha' p_t^2)^{\alpha-1} e_{00}^{\alpha+}(z_t) \xi_\alpha, \\ \phi_3^t + \phi_4^t &= \gamma_{+-}^{-2} t (\alpha' p_t^2)^{\alpha-1} [e_{11}^{\alpha+}(z_t) + z_t e_{11}^{\alpha-}(z_t)] \xi_\alpha, \\ \phi_3^t - \phi_4^t &= \gamma_{+-}^{-2} t (\alpha' p_t^2)^{\alpha-1} [z_t e_{11}^{\alpha+}(z_t) + e_{11}^{\alpha-}(z_t)] \xi_\alpha, \\ \phi_5^t &= \gamma_{++} \gamma_{+-} \sqrt{t} (\alpha' p_t^2)^{\alpha-1/2} [(1-z_t^2)^{1/2}] e_{10}^{\alpha+}(z_t) \xi_\alpha, \end{aligned} \quad (\text{A5})$$

where

$$\xi_\alpha = (1 \pm e^{-i\pi\alpha})/2 \sin\pi\alpha,$$

$$p_t^2 = \frac{1}{4}(t - 4m^2),$$

$$z_t = 1 + s/2p_t^2.$$

In the above expressions, we have also exhibited explicitly various properties of the Regge residues:

(i) factorization; (ii) the threshold behavior  $(\alpha' p_t^2)^{\alpha-1}$  appropriate for natural-parity trajectories (the scale parameter is chosen to be  $\alpha'$  to conform with dual models); (iii) a zero at  $t=0$  for the  $t$  channel flip residues. A quick way of seeing the origin of the latter is to consider, at  $t=0$ , the crossing relation

$$\phi_4^s(t=0) = \frac{1}{2}[(\phi_1^t - \phi_2^t) - (\phi_3^t - \phi_4^t)]. \quad (\text{A6})$$

Since conservation of angular momentum requires  $\phi_4^s(t=0) = 0$ , and since, for a natural-parity trajectory,  $\phi_1^t = \phi_2^t$ , it is necessary that  $\phi_3^t - \phi_4^t = 0$  at  $t=0$ . Since, for a natural-parity exchange,  $\phi_3^t = -\phi_4^t$  asymptotically, we conclude that  $\phi_3^t = \phi_4^t = 0$  at  $t=0$ . Factorization then implies a zero in the residues.

In the limit  $s \rightarrow \infty$ , fixed  $t$ , the known asymptotic behavior<sup>50</sup> of the functions  $e_{\lambda\mu}^{\alpha}$  implies (various common factors are absorbed in the residues)

$$\begin{aligned} \phi_1^t + \phi_2^t &\rightarrow \gamma_{++}^{-2} \frac{(\alpha' p_t^2 z_t)^\alpha}{\alpha' p_t^2} \xi_\alpha [1 + O(z_t^{-2})], \\ \phi_3^t - \phi_4^t &\rightarrow \frac{\gamma_{+-}^{-2} t}{2} \frac{(\alpha' p_t^2 z_t)^\alpha}{\alpha' p_t^2} \xi_\alpha [1 + O(z_t^{-2})], \\ \phi_3^t + \phi_4^t &\rightarrow \frac{\gamma_{+-}^{-2} t}{2} (\alpha' p_t^2 z_t)^{\alpha-1} \frac{2\alpha-1}{\alpha} \xi_\alpha [1 + O(z_t^{-2})], \\ \phi_5^t &\rightarrow \frac{\gamma_{+-} \gamma_{++} \sqrt{-t}}{2\sqrt{2}} \frac{(\alpha' p_t^2 z_t)^\alpha}{\alpha' p_t^2} \xi_\alpha [1 + O(z_t^{-2})]. \end{aligned} \quad (\text{A7})$$

Together with the crossing matrix these expressions allow us to write, at small  $t$ ,

$$\frac{U_0}{N_0} = \frac{\gamma_{+-}^2}{\gamma_{++}^2} \frac{2\alpha - 1}{\alpha} \frac{t}{z_t} \quad (\text{A8})$$

The above expression already exhibits the asymptotic suppression of natural-parity exchanges in  $U_0$ . The ratio  $\gamma_{+-}^2/\gamma_{++}^2$  can be obtained from estimates of  $N_1/N_0$  for a given trajectory. Let this ratio be

$$\frac{N_1}{N_0} = r \frac{\sqrt{-t}}{2m} \quad (\text{A9})$$

Use of the crossing matrix Eq. (A1) at small  $t$  yields

$$N_1 = -\frac{\sqrt{-t}}{4m} (\phi_1^t + \phi_2^t) - \phi_3^t, \quad (\text{A10})$$

$$N_0 = \frac{1}{2} (\phi_1^t + \phi_2^t). \quad (\text{A11})$$

Thus,

$$r \frac{\sqrt{-t}}{2m} = -\frac{\sqrt{-t}}{2m} - \frac{\sqrt{-t}}{\sqrt{2}} \frac{\gamma_{+-}}{\gamma_{++}},$$

or

$$\frac{\gamma_{+-}}{\gamma_{++}} = \frac{-1}{\sqrt{2m^2}} (1+r)$$

and

$$\frac{U_0}{N_0} = \frac{1-2\alpha}{\alpha} \frac{t}{2s} (1+r)^2. \quad (\text{A12})$$

If we treat the Pomeron as a factorizing  $t$ -channel pole, then we can use Eq. (A12) to estimate its contamination of the  $A_1$ -like amplitude  $U_0$ . Making the reasonable approximation  $r \ll 1$  (neglect helicity flip) and setting  $\alpha = 1$ , we find

$$U_0/N_0 \approx -t/2s. \quad (\text{A13})$$

Since this, or indeed the contribution of any factorizing natural-parity exchange vanishes at  $t=0$ , we conclude that the Pomeron contamination is not the source of  $\Delta\sigma_{\text{tot}}^L \sim -1$  mb at GeV/ $c$ . Of course, it is difficult to rule out a conspiracy, a nonfactorizing solution to the constraint equation  $\phi_3^t = \phi_4^t$  [Eq. (A6)] from which we deduced  $\gamma_{+-} \sim \sqrt{-t}$ . However, the cut models which are usually invoked to give conspiratorial solutions would give no contribution here since the  $s$ -channel helicity amplitudes  $\phi_1^s$  and  $\phi_3^s$  have no helicity flip.

We have investigated the consequences of adding a component  $(-t/2s)N_0$  to our  $A_1+Z$  estimate for  $U_0$  (purely real). Obviously, one still requires a large negative EXD-breaking imaginary part at  $t=0$  to explain  $\Delta\sigma_{\text{tot}}^L$ . Away from  $t=0$ , however, the Pomeron [Eq. (A13)] gives rise to a large positive imaginary part which contributes to  $C_{LL}$  as

$$C_{LL}\sigma/2K \propto -|N_0|^2(-t)/2s.$$

This is negative, as is the data (Fig. 7). Addition of a nonleading Pomeron component leads, therefore, merely to a reinterpretation of our phenomenological estimate of  $\text{Im}U_0$ —for which we have no model.

Naturality contamination also occurs in the reverse direction—i.e., nonleading unnatural-parity contributions can occur in  $N_0, N_1, N_2$  but, since these will behave as  $s^{\alpha_{UP}-\alpha_{NP}-1}$  relative to the leading contributions ( $\alpha_{NP} - \alpha_{UP} \sim \frac{1}{2}$  to  $\frac{3}{2}$ ) their effect is negligible.

#### APPENDIX B: THE COUPLING OF AN $A_1$ TRAJECTORY AT $t=0$

We show that the nonvanishing at  $t=0$  of the coupling of the  $A_1$ - $Z$  trajectories to  $N\bar{N}$  is consistent, to leading order in  $s$ , with the constraint  $\phi_4^s(t=0)=0$ .

From Eq. (A6) we find

$$\phi_4^s = \frac{1}{2}(\phi_1^t - \phi_2^t) - \frac{1}{2}(\phi_3^t - \phi_4^t) = 0. \quad (\text{B1})$$

For an  $L=J$  nucleon-antinucleon system such as the  $A_1$ ,

$$\phi_1^t = -\phi_2^t = 0. \quad (\text{B2})$$

Thus the constraint equation (B1) reduces to  $\phi_3^t - \phi_4^t = 0$ . However, for an unnatural-parity trajectory the linear combination  $\phi_3^t - \phi_4^t$  is zero to leading order in  $s$ .<sup>4</sup>

The above argument also can be extracted directly from Eq. (132) of Ref. 4(b) if we note that

$$d_{1-1}^J(z_t) + d_{11}^J(z_t) \underset{z_t \rightarrow \infty}{\sim} z_t^{J-1}. \quad (\text{B3})$$

In Ref. 4(a) the vanishing of the  $A_1$  coupling at  $t=0$  appears to be required by analyticity at  $t=0$ . Again, it can be verified that, to leading order in  $s$ , no unwanted singularity arises.

#### APPENDIX C: ELECTROMAGNETIC CORRECTIONS

We include electromagnetic corrections to  $pp$  elastic scattering by adding the contribution of one-photon exchange to the five helicity amplitudes. For small  $t$ , we derive

$$\begin{aligned} \phi_1 &= \phi_3 = 2e^2 \frac{s}{t} F_1^2, \\ \phi_2 &= -\phi_4 = 2e^2 \frac{s}{t} \frac{t}{4m^2} \kappa^2 F_2^2, \\ \phi_5 &= 2e^2 \frac{s}{t} \frac{\sqrt{-t}}{2m} \kappa F_1 F_2, \end{aligned} \quad (\text{C1})$$

where  $4\pi/e^2 \approx 137$ ,  $\kappa \approx 1.79$  is the anomalous magnetic moment of the proton and  $F_1$  and  $F_2$  are standard electromagnetic form factors. We use the empirically satisfactory parametrization,<sup>51</sup>

$$F_1 \approx F_2 = (1 - t/0.71)^{-2}.$$

We remark that the electromagnetic terms are real. They contribute to the polarization through interference with the imaginary part of the Pomeron. The contribution is positive but is subject to ambiguities associated with uncertainties in the phase of the Pomeron amplitude.

We would also remark that it is not altogether clear that we should add the photon-exchange terms in Eq. (C1) to our purely hadronic amplitudes. This question of principle arises because hadronic  $\rho$  exchange ( $\rho$  dominance) explains to a

large extent the anomalous magnetic moment of the proton. In the same spirit in which the photon-exchange term is used to extract the ratio of the real to imaginary part of  $(\phi_1 + \phi_3)$  from fits to  $d\sigma/dt$  at small  $t$ , we set aside this question of principle and add Eq. (C1) to our hadronic contributions.

In Fig. 4(c), we show that the Coulomb contribution to  $P$  at 100 GeV/c is considerable, accounting for 2% at very small  $t$  and  $\sim 0.5\%$  at intermediate values of  $|t|$ . Spin-dependent electromagnetic effects are discussed at length in Ref. 52.

<sup>1</sup>A. Yokosawa, Argonne Report No. ANL-HEP-PR-CP-47 (unpublished).

<sup>2</sup>P. Johnson, R. Miller, and G. Thomas, Phys. Rev. D **15**, 1895 (1977); A. B. Wicklund, in *Proceedings of the XVII International Conference on High Energy Physics, London, 1974*, edited by J. R. Smith (Rutherford Laboratory, Chilton, Didcot, Berkshire, England, 1974).

<sup>3</sup>M. Jacob and G. C. Wick, Ann. Phys. (N.Y.) **7**, 404 (1959); M. L. Goldberger *et al.*, Phys. Rev. **120**, 2250 (1960).

<sup>4</sup>(a) E. Leader and R. Slansky, Phys. Rev. **148**, 1491 (1966); (b) E. Leader, *ibid.* **166**, 1599 (1968).

<sup>5</sup>The precise properties of these combinations are discussed in the Appendix.

<sup>6</sup>L. Wolfenstein, Phys. Rev. **96**, 1654 (1954); C. Schumacher and H. Bethe, *ibid.* **121**, 1534 (1961); G. C. Fox, Caltech report, 1971 (unpublished); F. Halzen and G. Thomas, Phys. Rev. D **10**, 344 (1974).

<sup>7</sup>I. Ambats *et al.*, Phys. Rev. D **9**, 1179 (1974). For high-energy data, see D. S. Ayres *et al.*, *ibid.* **15**, 3105 (1977).

<sup>8</sup>R. Diebold *et al.*, Phys. Rev. Lett. **35**, 632 (1975); S. L. Kramer *et al.*, Phys. Rev. D **17**, 1709 (1978).

<sup>9</sup>D. R. Rust *et al.*, Phys. Lett. **58B**, 114 (1975); R. D. Klem *et al.*, Phys. Rev. D **15**, 602 (1977).

<sup>10</sup>M. Borghini *et al.*, Phys. Lett. **31B**, 405 (1970).

<sup>11</sup>D. Miller *et al.*, Phys. Rev. Lett. **36**, 763 (1976); G. Hicks *et al.*, Phys. Rev. D **12**, 2594 (1975).

<sup>12</sup>R. C. Fernow *et al.*, Phys. Lett. **52B**, 243 (1974); L. G. Ratner *et al.*, Phys. Rev. D **15**, 604 (1977); K. Abe *et al.*, Phys. Lett. **63B**, 239 (1976); H. E. Miettinen *et al.*, Phys. Rev. D **16**, 549 (1977); J. R. O'Fallon *et al.*, Phys. Rev. Lett. **39**, 733 (1977).

<sup>13</sup>I. P. Auer *et al.*, Phys. Lett. **70B**, 475 (1977).

<sup>14</sup>I. P. Auer *et al.*, Phys. Rev. Lett. **37**, 1727 (1976); A. Yokosawa (private communication).

<sup>15</sup>A. Yokosawa (private communication).

<sup>16</sup>R. C. Fernow *et al.*, Phys. Lett. **52B**, 243 (1974); L. G. Ratner *et al.*, Phys. Rev. D **15**, 604 (1977).

<sup>17</sup>G. W. Abshire *et al.*, Phys. Rev. D **12**, 3393 (1975); L. G. Ratner *et al.*, *ibid.* **15**, 604 (1977).

<sup>18</sup>J. Deregel *et al.*, Nucl. Phys. **B103**, 260 (1976).

<sup>19</sup>W. DeBoer *et al.*, Phys. Rev. Lett. **34**, 558 (1975).

<sup>20</sup>I. P. Auer *et al.*, Phys. Lett. **67B**, 113 (1977).

<sup>21</sup>G. C. Fox and C. Quigg, Annu. Rev. Nucl. Sci. **23**, 219 (1973); C. B. Chiu, *ibid.* **22**, 255 (1972).

<sup>22</sup>A. Irving and R. Worden, Phys. Rep. **34C**, 117 (1977).

<sup>23</sup>Recent data on  $\Delta\sigma_L$  (Ref. 20) have been interpreted

in terms of an isolated  $pp$  resonance in the  $^3F_3$  partial wave. K. Hidaka *et al.*, Phys. Lett. **70B**, 479 (1977). It is undeniable that there are substantial imaginary parts in certain  $pp$  amplitudes for  $p_{lab} < 3$  GeV/c. Nevertheless, we continue to work in the traditional framework in which the  $pp$  system is viewed as exotic.

<sup>24</sup>The extra signs arise because we use the Jacob and Wick "particle 2" convention.

<sup>25</sup> $\sigma_{tot}(\bar{p}p) > \sigma_{tot}(pp)$  implies  $\text{Im}\omega(pp) < 0$ ; since  $\sigma_{tot}(pp)$  is roughly constant with energy,  $\text{Im}f(pp) \approx -\text{Im}\omega(pp)$ .

<sup>26</sup>R. Carlitz, M. B. Green, and A. Zee, Phys. Rev. D **4**, 3439 (1971).

<sup>27</sup>For a recent phenomenological discussion, see A. Irving, Nucl. Phys. **B121**, 176 (1977).

<sup>28</sup>P. K. Williams, Phys. Rev. D **1**, 1312 (1970).

<sup>29</sup>G. Farmelo and A. C. Irving, Nucl. Phys. **B128**, 343 (1977).

<sup>30</sup>Recent analyses of diffractive production of the  $\rho\pi$  system suggest the existence of an  $A_1$  resonance; J.-L. Basdevant and E. L. Berger, Phys. Rev. D **16**, 657 (1977). An  $A_1$  enhancement is observed also in heavy-lepton decay  $\tau \rightarrow \rho\pi\nu$ , as reported in the talks by P. Lecomte and H. Meyer, meeting of the APS Division of Particles and Fields, Argonne, 1977 (unpublished).

<sup>31</sup>A. C. Irving and C. Michael, Nucl. Phys. **B82**, 282 (1974).

<sup>32</sup>Although amplitudes for  $A_1$  and  $Z$  exchange have been discussed previously in the literature, in the interests of self-consistency we provide more details for the  $A_1$  than for older, better studied trajectories. For previous investigations, consult Refs. 33-35.

<sup>33</sup>A. C. Irving, Phys. Lett. **59B**, 451 (1975).

<sup>34</sup>J. D. Kimel and J. F. Owens, Nucl. Phys. **B122**, 464 (1977).

<sup>35</sup>H. Haber and G. Kane, Nucl. Phys. **B129**, 429 (1977).

<sup>36</sup>A. C. Irving, Nucl. Phys. **B105**, 491 (1976).

<sup>37</sup>B. Renner, Phys. Lett. **21**, 453 (1966).

<sup>38</sup>It must be pointed out, however, that the same current algebra considerations imply an exceedingly large width for  $A_1 \rightarrow \rho\pi$  ( $\sim 500$  MeV) c.f. Ref. 37).

<sup>39</sup>J. Dash and H. Navelet, Phys. Rev. D **13**, 1940 (1976).

<sup>40</sup>M. M. Nagels *et al.*, Nucl. Phys. **B109**, 1 (1976).

<sup>41</sup>(a) J. A. Sheid *et al.*, Phys. Rev. D **8**, 1263 (1973). (b) A. Martin and H. Navelet, J. Phys. G (to be published).

<sup>42</sup>U. Amaldi, M. Jacob, and G. Matthiae, Annu. Rev. Nucl. Sci. **26**, 385 (1976).

<sup>43</sup>P. Jenni, *et al.*, Nucl. Phys. **B129**, 232 (1977).

- <sup>44</sup>R. D. Field and P. R. Stevens, Argonne Report No. ANL-HEP-CP-75-73, 1975 (unpublished).
- <sup>45</sup>Annecy-CERN-Oxford collaboration, preliminary data, obtained from D. Crabb (private communication).
- <sup>46</sup>H. Spinka, review talk at the 1977 Meeting of the American Physical Society Division of Particles and Fields, 1977 (unpublished); Argonne Report No. ANL-HEP-CP-77-80 (unpublished).
- <sup>47</sup>A. C. Irving, Nucl. Phys. B101, 263 (1975).
- <sup>48</sup>G. F. Chew, in *Antinucleon-Nucleon Interactions* (Pergamon, Oxford, 1976).
- <sup>49</sup>See, e.g., A. D. Martin and T. D. Spearman, *Elementary Particle Theory* (North-Holland, Amsterdam, 1970).
- <sup>50</sup>M. Gell-Mann *et al.*, Phys. Rev. 133, B145 (1964).
- <sup>51</sup>M. Goitein, J. R. Dunning, and R. Wilson, Phys. Rev. Lett. 18, 1018 (1967).
- <sup>52</sup>C. Bourrely and J. Soffer, Lett. Nuovo Cimento 19, 569 (1977); N. H. Buttimore, E. Gotsman, and E. Leader, Phys. Rev. D (to be published). See also E. Leader, Phys. Lett. 71B, 353 (1977).